Wood burning: A major source of Volatile Organic Compounds during wintertime in the Paris region

Baptiste Languille, Valérie Gros, Jean-Eudes Petit, Cécile Honoré, Alexia Baudic, Olivier Perrussel, Gilles Foret, Vincent Michoud, François Truong, Nicolas Bonnaire, et al.

Wood burning: a major source of Volatile Organic Compounds during wintertime in the Paris region

Baptiste Languille[1], Valérie Gros[1], Jean-Eudes Petit[1], Cécile Honoré[2], Alexia Baudic[2], Olivier Perrussel[2], Gilles Foret[3], Vincent Michoud[3], François Truong[1], Nicolas Bonnaire[1], Roland Sarda-Estève[1], Marc Delmotte[1], Anaïs Feron[3], Franck Maisonneuve[3], Cécile Gaimoz[3], Paola Formenti[3], Simone Kotthaus[4], Martial Haeffelin[4] and Olivier Favez[5]

[1]Laboratoire des sciences du climat et de l'environnement, CEA/Orme des Merisiers, 91191 Gif-sur-Yvette, France
[2]Airparif, Association agréée de surveillance de la qualité de l'air en Île-de-France, France
[3]LISA, UMR CNRS 7583, université Paris-Est-Créteil, université de Paris, Institut Pierre-Simon Laplace (IPSL), Créteil, France
[4]Institut Pierre-Simon Laplace, Centre national de la recherche scientifique, École polytechnique, 91128 Palaiseau, France
[5]Institut national de l'environnement industriel et des risques, Parc technologique ALATA, 60550 Verneuil en Halatte, France

Correspondence to: Baptiste Languille (baptiste.languille@lsce.ipsl.fr), Valérie Gros (valerie.gros@lsce.ipsl.fr)

Author contribution BL wrote the original draft, led data collection and processing and led the analysis. VG designed the campaign, gave a deep review on the first draft and participated in analysis. JEP participated in data processing, discussed analysis and reviewed the paper. CH, AB and OP discussed analysis, reviewed the paper and provided data (Airparif measurements and emission inventory). GF and VM discussed analysis, reviewed the paper and provided data (LISA measurements). FT participated in data processing. NB and RSE participated in data collection. MD provided data (CO measurements). AF and FM were involved in the deployment and maintenance of the instruments at LISA. CG was the technical manager for the EPPI project at LISA, she managed the installation and maintenance of the instruments. PF was the scientific manager of the PEGASUS platform where the measurements were conducted at LISA, she was in charge of the coordination of the platform use and instruments setup. SK reviewed the paper, SK and MH provided data (mixed layer height). OF supervised aerosol in situ measurements at SIRTA and reviewed the paper.

Abstract Wood burning is widely used for domestic heating and has been identified as a ubiquitous pollution source in urban areas, especially during cold months. The present study is based on a three and a half winter months field campaign in the Paris region measuring Volatile Organic Compounds (VOCs) by Proton Transfer Reaction Mass Spectrometry (PTR-MS) in addition to Black Carbon (BC). Several VOCs were identified as strongly wood burning-influenced (e.g., acetic acid, furfural), or traffic-influenced (e.g., toluene, C8-aromatics). Methylbutenone, benzenediol and butandione were identified for the first time as wood burning-related in ambient air.

A Positive Matrix Factorization (PMF) analysis highlighted that wood burning is the most important source of VOCs during the winter season. (47 %). Traffic was found to account for about 22 % of the measured VOCs during the same period, whereas solvent use plus background accounted altogether for the remaining fraction. The comparison with the regional

emission inventory showed good consistency for benzene and xylenes but revisions of the inventory should be considered for several VOCs such as acetic acid, C9-aromatics and methanol.

Finally, complementary measurements acquired simultaneously at other sites in Île-de-France (the Paris region) enabled evaluation of spatial variabilities. The influence of traffic emissions on investigated pollutants displayed a clear negative gradient from roadside to suburban stations, whereas wood burning pollution was found to be fairly homogeneous over the region.

1 Introduction

Wood burning presents several advantages for domestic heating. It is renewable, possibly produced locally, and considered as CO_2 neutral (Evtyugina et al., 2014). However, biomass burning is also known to be a major source of atmospheric pollutants, which has motivated scientific studies for years (Barrefors and Petersson, 1995a, b). Wood burning has been demonstrated to have deleterious health effects (e.g. Schwartz et al., 1996) related to the emission of particulate matter (PM, e.g., Fourtziou et al., 2017) and carcinogenic gaseous compounds such as benzene (e.g., Schauer et al., 2001; Bruns et al., 2017). For the Île-de-France (the Paris region), an emission inventory attributed 56 % of total emissions of PM below 1 µm in diameter (PM_1) and 12 % of the total Volatile Organic Compounds (VOCs) emissions to wood burning for residential heating (Airparif, 2019).

Previous studies focused on the impact of wood burning on air quality in Île-de-France, which unanimously highlighted the significance of this source. For instance, Favez et al. (2009) demonstrated that wood burning carbonaceous aerosols represent on average 20 % of the total $PM_{2.5}$ in Paris city during the winter season. Similar wintertime contributions to $PM_{2.5}$ (22-24 %) were obtained by Bressi et al. (2014) at different locations across Île-de-France. Moreover, wood burning was identified as responsible for about 30 % of the total carbonaceous matter, 35 % of Organic Aerosols (OA), 60 % of the combustion carbonaceous aerosols, and more than 20 % of total black carbon during winter at the SIRTA measurement site, located in the southern part of Île-de-France (Sciare et al., 2011; Crippa et al., 2013; Petit et al., 2014). Still, geographical origins are still an open question. The Paris region is known to be highly influenced by long-range transport of secondary pollutants (Freutel et al., 2013; Beekmann et al., 2015; Favez and Amodeo, 2016), but primary emissions can be considered as an important PM contributors during wintertime pollution episodes. OA was shown to be the main chemical species within the submicron aerosols for Île-de-France, with a large fraction being secondary organic aerosol (SOA) (Favez et al., 2007; Petit et al., 2015; Zhang et al., 2018). However, knowledge on SOA formation processes and origins is still incomplete (Ait-Helal et al., 2014). Recently, Bruns et al. (2016) underlined that wood burning has a strong potential to contribute to SOA formation through the emission of reactive VOCs. Based on simulation chamber experiments, they identified three main gaseous precursors (namely phenol, naphthalene and benzene) alone to be responsible for up to 80 % of the observed SOA concentration associated to wood burning. However, as other laboratory experiments using one wood burning appliance to identify and quantify emissions, the study suffered from a lack of reproducibility between burns, which can be

due to burning appliance efficiency and type (stove or fireplace), tree species, wood quality and humidity. Furthermore, real-world chemical interactions with other compounds emitted by various sources can only be investigated in ambient air.

Khalil and Rasmussen (2003) distinguished two ambient air tracers for biomass burning: chloromethane and the elemental carbon over organic carbon ratio. Gaeggeler et al. (2008) identified 17 VOCs as clearly associated with wood burning in an Alpine village. Baudic et al. (2016) conducted a source apportionment study in Paris city centre, examining one year (2010) of VOC measurements acquired at an urban background station. In winter, almost half of the measured VOCs were imputed to wood burning (Baudic et al., 2016); however, without taking into account the VOCs newly identified by Bruns et al. (2016) as strong SOA precursors.

In this context, the first goal of the present work was to identify, in ambient air, VOCs known as related to wood burning emissions and potentially important SOA contributors. This was achieved during a 3.5-month wintertime field campaign at a suburban site (SIRTA) representative of regional background conditions in the Paris area. Further, the objective was to quantify the respective wood burning and traffic contributions to VOC concentrations measured at this site by taking advantage of co-located measurements of other pollutants such as black carbon (BC), levoglucosan, nitrogen oxides (NO_x) and carbon monoxide (CO). The obtained source apportionment enabled a comparison with the regional emission inventory. Finally, complementary datasets obtained at other sites in Paris (suburbs and city centre) were used to investigated the BC, NO_x and VOCs spatial variations over the region.

2 Methods

2.1 SIRTA station

2.1.1 General description

The SIRTA (Site Instrumental de Recherche par Télédétection Atmosphérique[1]) is located 20 km southwest of Paris and is part of the European Aerosol, Clouds and Trace gases Research InfraStructure (ACTRIS[2]). This location is considered representative of suburban background conditions in Île-de-France (Haeffelin et al., 2005; Sciare et al., 2011).

This work uses observations gathered at the 5th zone of SIRTA, located at 5 km in the west of the SIRTA main site (latitude: 48.713 N, longitude: 2.208 E, the location map of all studied measurements is presented in Appendix A, Figure 1). The intensive campaign was conducted from 30 November 2017 to 12 March 2018. During this winter period temperatures were quite mild on average, but with large variations. According to the measurements at the Météo-France station of Toussus-le-Noble (5 km in the north-west of the station), with a mean air temperature of 7.1 °C January was warm compared to the long-term average (1981-2010) of 3.7 °C. In contrast, February was colder than usual, with a mean temperature of 1.2 °C compared to a long-term average temperature of 4.2 °C. These various conditions are favourable for the observation of both background, low-polluted periods and heavy wood burning influenced phases.

[1] http://sirta.ipsl.fr/, accessed on 10 April 2019
[2] https://www.actris.eu, accessed on 10 April 2019

2.1.2 VOC measurements by PTR-MS

As Proton Transfer Mass Spectrometer (PTR-MS) measurements at SIRTA constitutes the main dataset used in this study, the related acquisition and data treatment procedures are extensively detailed here; other VOC measurements at other stations are presented more briefly in Sections 2.2 and 2.3. The PTR-MS technique was developed in the 1990's by Lindinger et al. (1998). Numerous studies used this measurement technique afterwards; examples from diverse fields and details on the principle are given by de Gouw and Warneke (2007) and Blake et al. (2009).

A PTR-MS equipped with a quadrupole detector was used at SIRTA. A polytetrafluoroethylene (PTFE) line (inner diameter 0.030 in) kept at room temperature sampled ambient air from the rooftop (around 10 m above ground level). Masses from m/z 21 to 151 were scanned with a dwell time of 5 sec per mass, which led to a cycle of about 11 min. For consistency with other datasets, PTR-MS data were averaged to 15-min resolution (using the Openair package from R described on Section 2.7). The pressure (P_{Drift}), temperature (T_{Drift}), and voltage (V_{Drift}) of the reaction chamber were set respectively to 2.2 mbar, 60◦C and 600 V. This setup led to an E/N ratio of about 132 Td (1 Td = 10^{-17}.cm^2.V^{-1}).

A Gas Calibration Unit (GCU) from Ionicon Analytik was used for regular field blank measurements (during 1 hour, every 13 hours) and seven calibrations during the campaign. Calibrations were performed with a VOC mixture from Ionicon. Eleven protonated masses were considered: 33-methanol, 42-acetonitrile, 45-acetaldehyde, 57-propenal, 59-acetone, 69-isoprene, 71-crotonaldehyde, 73-butanone, 79-benzene, 93-toluene and 107-xylenes. The calibration was done following five concentration steps (1, 2, 4, 8 and 16 ppb) of one hour each. The transmission curve was used for the other masses quantification, according to the method suggested by Taipale et al. (2008) and the reaction rate constants given by Zhao and Zhang (2004). A target gas mixture (bottle of stable atmospheric sample) was measured once a week to assess the measurement stability with time. Uncertainties were calculated according to the ACTRIS guidelines (ACTRIS, 2014) for the calibrated masses. The mean uncertainties ranged from 13 % of the mean concentration for the m/z 59 to 35 % for the m/z 73 and 91 % for the m/z 107. For the "transmission masses", the uncertainty was estimated to be approximately 40 %. All detailed calculations are presented in Appendix B.

The PTR-MS used here participated successfully in an international intercomparison exercise shortly before the presented, with results provided by Holzinger et al. (2019).

In ambient air, 25 masses were considered, corresponding to the VOCs identified as a single VOC or a group of VOCs (Table 1), characterized by the highest signal-to-noise ratio. As a quadrupole was used, the measurement is related to a unitary mass and it cannot be ruled out that a compound effectively measured was not taken into account. Hence the "used name" should be considered as the most likely or major compound, and not as a certain identification. Still, most of the compounds are known to be the majority at a given mass (methanol, acetonitrile, benzene, toluene, etc.) The mass 43 was identified as related to propene, but as several other fragments are also measured at the same mass, the label "propene+" was chosen. m/z 69 is often associated to isoprene but this compound is mainly emitted by biogenic sources, which can be

considered negligible in the Paris area during winter (Baudic et al., 2016). This assumption was affirmed by the diurnal cycle observed for this m/z, which is not associated with a typical biogenic pattern (Appendix J). In the context of the present study, m/z 69 could be considered to be mostly related to furan. For masses where no evidence for the association with a specific preferential compound was found, the used name was assigned according to the most abundantly emitted compound in the Bruns et al. (2017) study (e.g., furfural instead of dimethylfuran for the m/z 97).

Used name	m/z	Related compound(s)
Formaldehyde	31	Proxy-formaldehyde
Methanol	33	Methanol
Acetonitrile	42	Acetonitrile
Propene+	43	Propene = propylene, several fragments
Acetaldehyde	45	Acetaldehyde
Propenal	57	Propenal = acrolein, butanol
Acetone	59	Acetone, propanal
Acetic acid	61	Acetic acid, propanol, glycolaldehyde
Furan	69	Furan, isoprene, cyclopentene
Butenal	71	Crotonaldehyde = butenal, methyl vinyl ketone, methacrolein, pentene, methylbutene
MEK	73	Butanone = methyl ethyl ketone, butanal, methylpropanal, methylglyoxal
Methylacetate	75	Methylacetate, hydroxyacetone
Benzene	79	Benzene
Hexenal + monoterp.	81	Hexenal, monoterpenes
Methylfuran	83	Methylfuran, hexenol, hexanal
Methylbutenone	85	Ethyl vinyl ketone, methylbutenone
Butandione	87	Butandione
Toluene	93	Toluene
Phenol	95	Phenol, Vinylfuran
Furfural	97	Furfural = furfuraldehyde, dimethylfuran
Furandione	99	Furandione
C8-arom.	107	Xylenes, ethylbenzene, benzaldehyde
Benzenediol	111	Benzenediol, methylfuraldehyde

Chlorobenzene	113	Chlorobenzene
C9-arom.	121	Trimethylbenzene, ethylmethylbenzene, propylbenzene, methylbenzaldehyde, phenylethanone

Table 1 25 considered VOCs during the field campaign at SIRTA. The identification of the masses was done with the review articles by Blake et al. (2009) and de Gouw and Warneke (2007) for the most commonly measured VOCs, and with other studies for more specific compounds (Kim et al., 2009; Baasandorj et al., 2015; Bruns et al., 2017).

2.1.3 Other measurements at SIRTA

An Aethalometer (AE33 model, Magee Scientific) has been monitoring BC continuously at SIRTA at 1-min resolution. The 7-wavelength measurements not only allowed to estimate total black carbon concentrations but also to roughly apportion the contribution of the two major BC sources: fossil fuel and biomass burning (Drinovec et al., 2015). This source apportionment model was developed by Sandradewi et al. (2008) and was successfully used in numerous studies afterwards (e.g., Favez et al., 2009; Sciare et al., 2011; Petit et al., 2014, 2015; Kalogridis et al., 2018). Based on these studies, the two BC fractions were used here as tracers for traffic ($BC_{traffic}$) and wood burning (BC_{wb}) emissions, respectively.

Validation of AE33 data, as well as the optimization of the BC model are detailed in Appendix C. Levoglucosan, a well-known tracer of biomass combustion (Puxbaum et al., 2007), was measured on a daily basis during the campaign. Its correlation with BC_{wb} reached 0.90. NO_2 measurements (commonly strongly associated with traffic) were also conducted at SIRTA; the correlation with $BC_{traffic}$ is 0.85. These excellent correlations strengthen the validity of the BC source apportionment.

Nitrogen monoxide (NO) and nitrogen dioxide (NO_2) were measured at SIRTA by chemiluminescence using a T200UP (Teledyne) equipped with a blue light photolytic converter. Ozone (O_3) was measured using a T400 (Teledyne), based on ultraviolet absorption. The initial measurements at 1-minute resolution were averaged to 15 minutes to match the other measurements' time step. Most of data processing and figures were done using the R language (R Core Team., 2018) and particularly the Openair package, designed by Carslaw and Ropkins (2012).

Levoglucosan was measured following the technique reported by Iinuma et al. (2009), using a DIONEX ICS 3000 system equipped with an Electrochemical detector and gold electrode. The separation was performed using a Dionex CarboPac MA1 4-mm diameter column. Eluent type, concentrations, and gradients were similar to those reported by Iinuma et al. (2009). Punches of 10.51 cm^2 of QMA filter samples were placed into rinsed plastic vials containing 10 ml of mQ water and were extracted by sonication for 45 min. Extracted liquid samples were immediately filtered (0.20 µm pore size diameter Teflon filter) and analysed for their content (including levoglucosan). Linear calibration (with r^2 better than 0.99) was obtained with standard concentrations ranging 10 ppb to 1 ppm allowing the quantification of levoglucosan at pbb levels. This same technique was used in previous studies, such as Bressi et al. (2014).

Finally, 1-min average CO measurements were obtained from continuous monitoring (at 3 seconds), performed at the Saclay tower with a PICARRO instrument (based on a Cavity Ring Down Spectroscopy technique, model G2401). The Saclay tower (latitude: 48.723 N, longitude: 2.142 E) belongs to the French National atmospheric monitoring network for greenhouse gases and is also part of the ICOS (Integrated Carbon Observation System) European Network and research infrastructure[3]. It is a 100 m high tower equipped with three sampling heights that are measured sequentially every 20 min. Data are processed in near-real time by ICOS following the protocol described in Hazan et al. (2016).

2.2 LISA laboratory

Data obtained at the LISA laboratory from 2 February to 12 March 2018 was also used in the present study. This laboratory is located in the city of Créteil, 10 km southeast of Paris city centre in a dense urban area, and a few hundred meters away from a major highway. Instruments for BC, NO_x and VOC measurements are part of the PEGASUS (PortablE Gaz and Aerosol Sampling UnitS) mobile platform[4].

VOC measurements were conducted with a PTR-ToF-MS (KORE Inc. 2nd generation). Twenty protonated masses were extracted from the instrument among which ten were calibrated and led to quantification. Ambient air was sampled through a 5 m long Teflon line with a flow rate of 3 $L.min^{-1}$ and through a glass manifold. The PTR-ToF-MS was connected to the manifold with a 1 m long silcosteel line heated to 60°C with a sampling flow rate of 300 $mL.min^{-1}$. The instrument was operated at a reactor pressure of 2.0 mbar and a temperature of 60 °C leading to an E/N ratio of 140 Td. An automated zero procedure was performed every hour for 10 min. Humid zero air was generated by passing ambient air through a catalytic converter. The PTR-ToF-MS was calibrated before and after the campaign at various relative humidity levels using a Gas Calibration Unit (IONICON). Signals of every mass were accumulated over 10 min and normalized by the signals of H_3O^+ and the first water cluster $H_3O^+(H_2O)$ as proposed by de Gouw and Warneke (2007). A factor was also introduced to account for the effect of humidity on the PTR-ToF-MS sensitivity. It was determined experimentally performing calibrations at various relative humidity.

NO_x measurements were performed using an ozone chemiluminescence monitor (APNA-370 from HORIBA) with a heated Molybdenum catalytic converter.

BC measurements were conducted with an Aethalometer (AE31 from Magee Scientific) sampling at 2 $L.min^{-1}$ from a high-volume total suspended particulate inlet. This Aethalometer uses 7-wavelengths allowing the distinction of fossil fuel or wood burning origin of BC. The same methodology as used at SIRTA was applied for the data correction, validation and apportionment of traffic and wood burning fractions of BC (Appendix C).

2.3 Airparif stations

[3] www.icos-ri.eu, accessed on 10 April 2019
[4] http://www.pegasus.cnrs.fr/, accessed on 4 July 2019

Airparif is the organization approved by the French Ministry of Environment to monitor air quality in Île-de-France[5]. For the present work, continuous VOC, BC and NO_x measurements were made available. The VOC measurement site is located on the roof of the main Airparif building, close to busy roads, in the Paris city centre. The measurements have been performed with an On-line Turbomatrix Gas-Chromatography Mass Spectrometry from PerkinElmer (Baudic et al., 2016). Co-located BC and NO_x measurements are notably conducted at two urban background (Gennevilliers and Paris XIII^e) and three traffic (Boulevard Haussmann, Highway A1 and Ring road east) sites. BC measurements were achieved using the AE33 instrument, and data were processed as presented in Section 2.1.3. For traffic sites, absolute values of BC_{wb} concentrations were disregarded as they were expected to be associated with high uncertainties in these locations heavily impacted by vehicular exhaust emissions. NO_x measurements were performed using two different instruments, both based on chemiluminescent technology: an AC32 EN from Environment SA and a Model 42i from Thermo Fisher Scientific, both equipped with a Molybdenum catalytic converter.

2.4 Meteorological data

Air masses back-trajectories were calculated with the Hybrid Single Particle Lagrangian Integrated Trajectory Model (HYSPLIT) (Stein et al., 2015; Rolph, 2016). The trajectories' end was set at SIRTA (latitude: 48.709, longitude: 2.149) at 10 m above ground level in order to match the sampling conditions. These trajectories were calculated for 96 hours at 3-hour intervals.

Mixed layer height (MLH) data were derived from attenuated backscatter profile observations collected with a Vaisala CL31 ceilometer at SIRTA. Raw data were corrected following the methods outlined by Kotthaus et al. (2016) before the automatic CABAM algorithm (Kotthaus and Grimmond, 2018) was applied to determine MLH, block-averaged to 15 min intervals. Subsequent quality control (Kotthaus et al., in prep) ensured unreasonable results were excluded from analysis.

Additional meteorological data (temperature, wind speed and wind direction) were provided by Météo-France for three stations. Monthly mean data were used for the Toussus-le-Noble station (located 5 km away from SIRTA), and hourly mean data for the Montsouris station (located in a public garden in Paris centre) and for the Saint-Maur station (3 km away from LISA).

For consistency, all data have been averaged upon a 15-min time-base.

2.5 Emission inventory

The emission inventory from Airparif was examined in this study. The latest version used here is representative of the emissions in 2015 (Airparif, 2019). This inventory differentiates the ten following pollutant source categories, called SNAP (for Selected Nomenclature for Air Pollution) according to the European Monitoring and Evaluation Programme (EMEP, 2016): 1-Combustion in energy and transformation industries, 2-Non-industrial combustion plants, 3-Combustion in manufacturing industry, 4-Production processes, 5-Extraction and distribution of fossil fuels and geothermal energy, 6-

[5] www.airparif.asso.fr, accessed on 10 April 2019

Solvent and other product use, 7-Road transport, 8-Other mobile sources and machinery, 9-Waste treatment and disposal and 10-Agriculture. An eleventh group gathering other sources (especially natural emissions) and sinks was taken into account in the Airparif inventory.

This inventory was based on emission profiles for each source given by the Interprofessional Technical Centre for Studies on Air Pollution (CITEPA[6]) and the Institute for Energy Economics and the Rational Use of Energy (IER)[7] . The profiles were established based on numerous research studies. For the version of the inventory used here, 145 emission profiles concerning 521 VOCs were considered. More details are given in the methodological guidelines (Airparif, 2019).

All SNAP are composed of sub-groups. For comparison purposes, four bins were used in the present study. They are relevant for the following sources: wood burning (SNAP 020201 and SNAP 020202 for the combustion plants, SNAP 020204 for the stationary engines and SNAP 020205 for other equipment such as stoves, fireplaces, cooking, etc.), traffic (SNAP 07 for road transport including cars, duty vehicles, motorcycles, etc.) and solvent use, both industrial and domestic (SNAP 06 including different solvent and painting applications). The fourth bin gathered all the other emissions sources. In order to make the comparison pertinent, the wintertime period of the inventory was considered (i.e. January, February, and March).

2.6 Positive matrix factorization (PMF)

Positive Matrix Factorization (PMF) was used for the source apportionment of VOCs measured at SIRTA as described in Appendix D. PMF is a statistical receptor model for source apportionment developed by Paatero and Tapper, (1994). It is now widely used in the field of atmospheric chemistry, for both particulate matter (Petit et al., 2014; Petit et al., 2015; Maenhaut, 2018) and for gas-phase compounds (Lanz et al., 2008; Buzcu-Guven and Fraser, 2008; Sauvage et al., 2009; Gaimoz et al., 2011; Baudic et al., 2016; Debevec et al., 2017; Bari and Kindzierski, 2018).

The principle is to decompose the input data (measurement time series, named X) into two matrices: factor profile (the chemical composition of each factor, named F) and the temporal contribution at each time step (matrix G). The model is based on the following formula:

$$x_{ij} = \sum_{p=1}^{k} g_{ip} \cdot f_{pj} + e_{ij}$$

Where x_{ij} is the concentration of compound j at time step i, g_{ip} is the contribution of the factor p at the time step i, f_{pj} is the contribution of the factor p to the compound j, k is the number of factors and e_{ij} are the residuals corresponding to the part not explained by the model.

[6] https://www.citepa.org/en/activities/emission-inventories, accessed on 10 April 2019
[7] http://www.ier.uni-stuttgart.de, accessed on 10 April 2019

The 25 VOCs presented in Table 1 were considered for the analysis conducted using the EPA PMF 5.0. The uncertainties used for the PMF model were harmonized for calibrated and non-calibrated VOCs, according to Ito et al. (2004), i.e. 5 % of the concentration plus the detection limit. The PMF analysis led to a 3-factor solution, as described in Appendix D.

3 Results

3.1 Overview of the results obtained at SIRTA

Figure 1 summarizes the results obtained from VOCs and BC measurements at SIRTA. The predominant VOCs were methanol, acetone, propenal, acetic acid as well as aromatics (benzene, toluene, C8-arom. and C9-arom.), together representing 75 % of the total VOC measured mass (values are presented in Appendix E, Table E1). This is consistent with previous studies performed in Paris where methanol and acetone were the most abundant species (Gros et al., 2011; Baudic et al., 2016), mainly emitted by natural sources and solvent use.

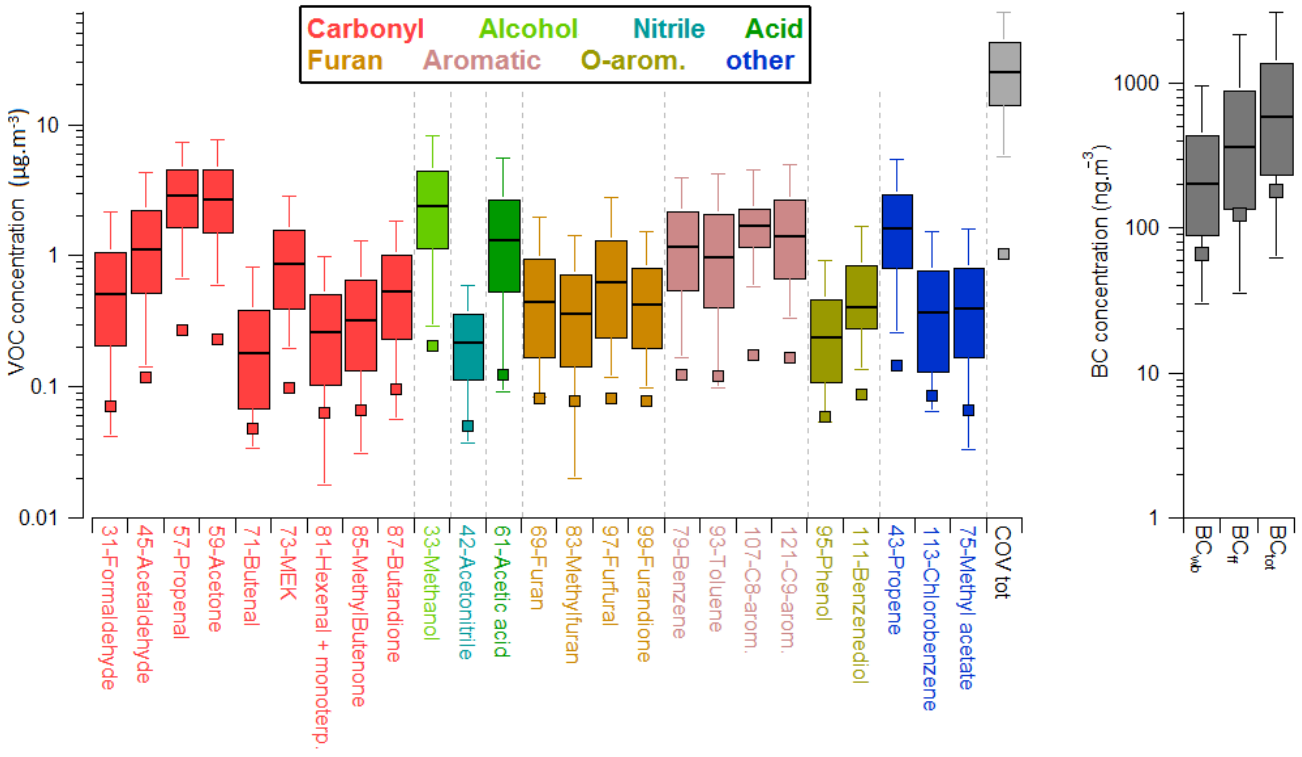

Figure 1 Distribution of BC (ng.m^{-3}) and VOC (µg.m^{-3}) measurements during the campaign. Boxes represent 25th and 75th percentiles, the black line is the median. Whiskers represent 5th and 95th percentiles. The squares represent the mean value during the "background" period from 15 to 25 January 2018.

Comparisons with other studies located at SIRTA (Ait-Helal et al., 2014), in Paris city centre (Baudic et al., 2016) and in European places (Seco et al., 2013 for Barcelona, Spain and Valach et al., 2014 for London, UK) were conducted (values are available in Appendix F, Figure F1 and Table F1). The mean concentrations measured here are systematically lower than the

ones obtained by Ait-Helal et al. (2014), although the two sampling sites are very close to each other. The difference is mainly due to the different considered period as the Ait-Helal et al. study was from mid-January to mid-February 2010 and these two months were associated with colder temperature than the present study (2 °C and 3.5 °C below normal values for January and February, respectively).

As expected, when taking into account the site locations, all the VOC concentrations acquired for this study at SIRTA were lower than the loadings commonly measured at dense urban places. The measurements done by Baudic et al. (2016) in Paris city centre during wintertime showed much higher concentrations for all the VOCs. This is particularly true for aromatics; benzene concentration was twice as high, and toluene and C8-arom. were more than four times more abundant than in this study. Values reported by Valach et al. (2014) for London were dramatically higher than at SIRTA. On the contrary, SIRTA showed levels very close to the observations reported by Seco et al. (2013) at Montseny (rural area).

Time series of a selection of VOCs are presented in Appendix G (Fig), showing substantial contrasts between background levels and polluted episode. While most pollution episodes were characterized by a strong traffic influence (high $BC_{traffic}$ concentration), several were associated with an important wood burning impact. At times, BC_{wb} was even higher than $BC_{traffic}$, which is rarely seen at SIRTA (Petit et al., 2014; Petit et al., 2015). As detailed in Appendix H (Figure H1), these differences between low and high-polluted periods were mainly driven by meteorological parameters (air mass origin, wind, temperature and mixed layer height).

This contextualisation confirms the suburban typology of SIRTA (representative of regional background with occasional polluted episodes). Note that the spatial variabilities of pollutant concentrations are further discussed in Section 3.4 of the present paper.

3.2 Qualitative investigation of wood burning and traffic influences at SIRTA

Wood burning and traffic influences on VOC loadings were qualitatively investigated according to two different methods. The first one is derived from a methodology designed by Gaeggeler et al. (2008) which is based on correlations between VOC and specific tracers as well as on relevant ratios described below. The second method used to discriminate wood burning from traffic compares the average diurnal cycle of each VOC to typical, previously established reference patterns.

3.2.1 VOC classification as wood burning or traffic influenced

Gaeggeler et al. (2008) performed a study based on VOC measurements acquired in Roveredo, an Alpine village in southern Switzerland. To associate VOCs either to wood burning or traffic, they designed a methodology composed of four parameters: the correlation coefficient between the mean diurnal cycles of VOC and CO, the latter being a known combustion tracer; the correlation coefficient between the mean diurnal cycles of VOC and NO_x, which is mostly emitted by traffic; the night (N) over morning (M) concentration ratio (N/M), which is expected to be high for wood burning-related pollutants (mostly emitted in the evening) and low for traffic-related pollutants (because of the important emissions during

the morning rush hours); and the weekday over Sunday concentration ratio (W/S) for the morning hours (based on the hypothesis of particularly significant wood burning activities and a very weak traffic flow on Sunday morning).

In our study, representative hours during morning and night were selected to coincide with dominant human activities in the area, i.e. peak hours for traffic and wood burning pollution: night hours were chosen from 23:00 to 02:00 local time, and morning hours from 08:00 to 11:00 local time. All the correlations calculated are the Pearson correlation coefficient. The ratio between the CO correlation (r_{CO}) and the NO_x correlation (r_{NOx}) was considered instead of r_{NOx} and r_{CO} separately, in order to reinforce the distinction. Also, r_{BCwb} and $r_{BCtraffic}$ were added to the methodology.

As outlined below, the weekdays over Sunday ratio (W/S) did not give satisfying results and was therefore not taken into account for the classification. Hence, the following parameters were for the VOC classification: r_{CO} / r_{NOx}, N/M, r_{BCwb}, and $r_{BCtraffic}$.

Wood burning	$r_{CO}/r_{NOx} > 2$	N/M >1	$r_{BCwb} > 0.80$	$r_{BCtraffic} < 0.45$
Traffic	$r_{CO} / r_{NOx} < 0.5$	N/M < 0.9	$r_{BCwb} < 0.45$	$r_{BCtraffic} > 0.80$

Table 2 Parameters thresholds for VOC classification. r_{NOx}: correlation coefficient with the diurnal cycle of NO_x; r_{CO}: correlation coefficient with the diurnal cycle of CO; N/M: night over morning concentration ratio; W/S: weekday over Sunday concentration ratio; r_{BCwb}: correlation coefficient with BC_{wb}; $r_{BCtraffic}$: correlation coefficient with $BC_{traffic}$.

The thresholds chosen for these four criteria (Table 2), gave the most distinct separation between the two sources. Each VOC was classified as wood burning or traffic-related if all respective criteria were fulfilled. The VOCs classified as either wood burning or traffic-related are listed in Tables 5 and 6, respectively. It is worth noting that this classification does not take into account potential multi-source origins of these compounds but rather assigns each compound to its dominating source.

The method classified 14 VOCs to originate predominantly from wood burning. The most correlated compounds with BC_{wb} were furan, furfural and methanol (with r of 0.96, 0.96 and 0.94), all presenting poor correlations with $BC_{traffic}$ (max 0.13) and with NO_x (max 0.23). Methanol was further characterized by one of the lowest weekdays over Sunday ratio (0.89). Furan had the highest correlation with CO (r = 0.79). Furfural had the highest night over morning ratio (1.78) and was highly correlated with CO (r = 0.77). The attribution of these three VOCs to wood burning sources is hence particularly robust.

Three VOCs were associated with traffic: toluene, C8-arom. and C9-arom. They showed a high correlation with $BC_{traffic}$ (more than 0.82), a low correlation with CO (less than 0.28), as well as a low night over morning ratio (less than 0.84). It should be noted that the correlation with BC_{wb} was low for C8-arom. (0.22) but not negligible for toluene and C9-aromatics (0.40 and 0.42), which may suggest a small contribution of the wood burning source.

VOC	m/z	r_{NOx}	r_{CO}	r_{CO} / r_{NOx}	N/M	W/S	r_{BCwb}	$r_{BCtraffic}$
Methanol	33	0.21	0.73	3.48	1.18	0.89	0.94	0.13
Acetonitrile	42	0.03	0.69	23.00	1.17	1.01	0.86	-0.07
Propene+	43	0.28	0.59	2.11	1.16	1.21	0.84	0.24
Propenal	57	0.21	0.59	2.77	1.06	0.90	0.83	0.24
Acetic acid	61	0.05	0.73	14.60	1.77	1.67	0.91	-0.07
Furan	69	0.23	0.79	3.43	1.28	0.88	0.96	0.11
Methylacetate	75	0.09	0.70	7.78	1.55	0.87	0.92	0.00
Methylfuran	83	0.34	0.68	2.00	1.16	0.89	0.89	0.25
Methylbutenone	85	0.22	0.70	3.18	1.36	1.05	0.92	0.14
Butandione	87	0.21	0.72	3.43	1.31	1.04	0.93	0.10
Furfural	97	0.14	0.77	5.50	1.78	0.91	0.96	0.03
Furandione	99	0.04	0.66	16.50	1.52	1.18	0.85	-0.08
Benzenediol	111	0.18	0.75	4.17	1.42	0.95	0.90	0.06
Chlorobenzene	113	0.14	0.61	5.64	1.27	1.10	0.84	0.10

Table 3 14 VOCs classified as wood burning related. VOC: compound associated with the mass; m/z: protonated mass; r_{NOx}: correlation coefficient with the diurnal cycle of NO_x; r_{CO}: correlation coefficient with the diurnal cycle of CO; r_{CO} / r_{NOx} is the correlation ratio; N/M: night over morning concentration ratio; W/S: weekday over Sunday concentration ratio; r_{BCwb}: correlation coefficient with BC_{wb}; $r_{BCtraffic}$: correlation coefficient with $BC_{traffic}$.

335

VOC	m/z	r_{NOx}	r_{CO}	r_{CO} / r_{NOx}	N/M	W/S	r_{BCwb}	$r_{BCtraffic}$
Toluene	93	0.81	0.27	0.33	0.81	0.91	0.40	0.88
C8-arom.	107	0.80	0.07	0.09	0.75	1.16	0.22	0.88
C9-arom.	121	0.75	0.28	0.37	0.84	1.06	0.42	0.82

Table 4 3 VOCs classified as traffic-related. VOC: compound associated with the mass; m/z: protonated mass; r_{NOx} : correlation coefficient with the diurnal cycle of NOx; r_{CO}: correlation coefficient with the diurnal cycle of CO; r_{CO} / r_{NOx} is the correlation ratio; N/M: night over morning concentration ratio; W/S: weekday over Sunday concentration ratio; r_{BCwb} : correlation coefficient with BC_{wb}; $r_{BCtraffic}$: correlation coefficient with $BC_{traffic}$.

Some general features of the used parameters were found that indicate qualitative VOC classification into wood burning or traffic-related. Wood burning VOCs had a correlation with NO_x lower than 0.34 while it was higher than 0.75 for traffic-related VOCs. Correlations with CO were higher than 0.59 for wood burning VOCs and lower than 0.28 for traffic VOCs. Correlations with BC_{wb} were higher than 0.83 for wood burning VOCs and lower than 0.42 for traffic VOCs; r with $BC_{traffic}$ were lower than 0.25 for wood burning VOCs and higher than 0.82 for traffic VOCs. The night over morning ratio was also a discriminant parameter with all the wood burning VOCs higher than 1.06 and the traffic VOCs lower than 0.84. The weekdays over Sunday ratio was the least relevant parameter, as values for wood burning (0.87 - 1.67) and traffic VOCs (0.91 - 1.16) were very similar. This is likely explained by either (or both) a non-negligible traffic activity or moderate wood burning activity on Sunday mornings.

Eight VOCs were classified neither as wood burning nor traffic-related: formaldehyde, acetaldehyde, acetone, butenal, MEK, benzene, hexenal + monoterp. and phenol. This suggests either a double influence (both traffic and wood burning contributions) or a dominating third source.

3.2.2 Diurnal cycles

Wood burning and traffic activities in the area have distinct diurnal patterns. Figure 2 (panel A) shows the diurnal cycle of the accumulated traffic jam length over the Île-de-France region for the studied period. This metric is interpreted as a traffic intensity marker, with two peaks illustrating the rush hours during morning (centred at 7:00 UTC) and evening (centred at 17:00 UTC), respectively.

The accumulated traffic jam length shows repeated peaks for each working day. The morning and evening peaks had a similar intensity from Monday to Friday and a different pattern during weekends, with a unique, smaller peak in the afternoon. However, the time series of the traffic tracer $BC_{traffic}$ show different variations, with no clear or repeating diurnal cycle (a two-week sample is presented in Appendix I, Figure I1). This is due to additional processes driving the observed concentration such as wind and rain.

Despite this high day-to-day variability, the diurnal cycle of $BC_{traffic}$ averaged over the whole campaign reveals a clear pattern (Figure 2, panel B). The two daily peaks of the average cycle of $BC_{traffic}$ match those seen for the accumulated traffic jam length (~ 07:00 and ~ 17:00 UTC). The diurnal pattern of BC_{wb} has only one extended peak during evening, occurring later than the traffic peak (centred on 19:00 UTC) and lasting longer (from 17:00 to 22:00 UTC).

The VOC diurnal cycles are also typical (Figure 2, panel C). The toluene cycle is characterized by two peaks following the typical traffic pattern, while the methanol diurnal cycle is defined by only one peak later in the evening, as seen for the wood burning signal. Benzene showed two peaks but the evening one is higher and occurs later. This suggests that toluene is strongly traffic-influenced, methanol is strongly wood burning-influenced and benzene is associated with both sources.

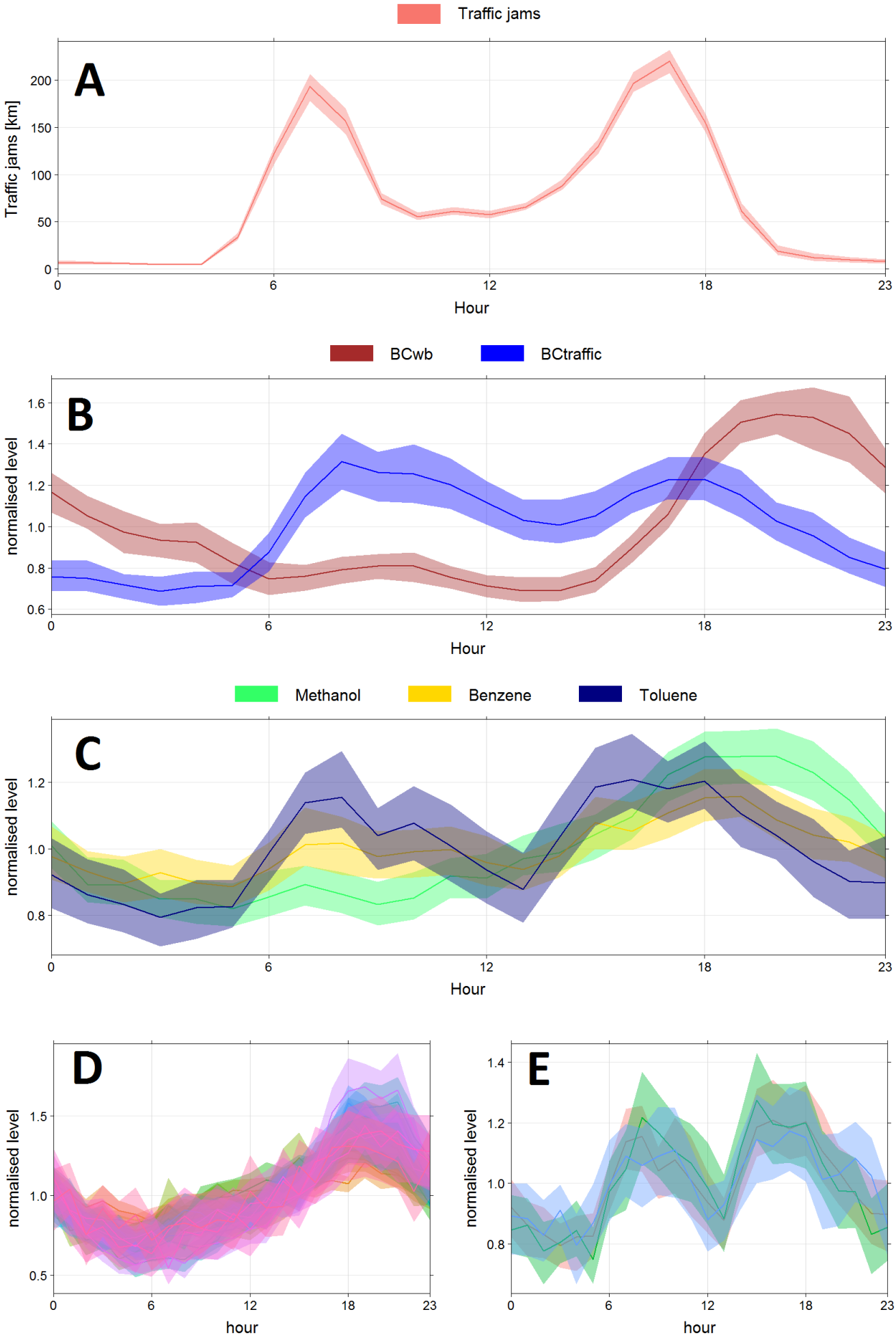
Traffic jams
A
Traffic jams [km]
0
50
100
150
200
0
6
12
18
23
Hour
BCwb
BCtraffic
B
normalised level
0.6
0.8
1.0
1.2
1.4
1.6
0
6
12
18
23
Hour
Methanol
Benzene
Toluene
C
normalised level
0.8
1.0
1.2
0
6
12
18
23
Hour
D
normalised level
0.5
1.0
1.5
0
6
12
18
23
hour
E
normalised level
0.8
1.0
1.2
1.4
0
6
12
18
23
hour

Figure 2 Diurnal cycles for the whole studied period (31 November 2017 to 12 March 2018) at SIRTA. The shaded area represents two standard deviations, hours are in UTC. Panel A: cumulated traffic jams length across Île-de-France. Panel B: BC_{wb} and $BC_{traffic}$. Panel C: toluene, benzene and methanol. Panel D: VOC associated with a wood burning pattern (formaldehyde, methanol, acetonitrile, propene+, acetaldehyde, acetic acid, furan, butenal, methylacetate, methylfuran, methylbutenone, butandione, furfural, furandione, benzenediol and chlorobenzene). Panel E: VOC associated with a traffic pattern (toluene, C8-arom. and C9-arom).

The diurnal cycle analysis provides a qualitative reference regarding of the dominant source of each VOC, according to comparison to the wood burning pattern (only one wide late evening peak) or the traffic pattern (two peaks a day). Figure 2 (panels D and E) presents the VOC diurnal cycles, either characterized by the wood burning or traffic pattern. Sixteen VOCs were defined by a wood burning pattern: formaldehyde, methanol, acetonitrile, propene+, acetaldehyde, acetic acid, furan, butenal, methylacetate, methylfuran, methylbutenone, butandione, furfural, furandione, benzenediol and chlorobenzene. They are plotted individually in Appendix J, Figure J1. Among them, there are all the VOCs classified as wood burning-related by the four-parameter method (Section 3.2.1) except for propenal. Three additional VOCs (formaldehyde, acetaldehyde and butenal) followed this wood burning pattern, although they were not associated with this source by the statistical parameters method.

Three VOCs were characterized by the traffic pattern: toluene, C8-arom. and C9-arom. (plotted individually in Appendix J, Figure J2), confirming the results discussed in Section 3.2.1.

Based on the diurnal cycle, six VOCs were not classified as being dominated by either wood burning or traffic emissions: propenal, acetone, MEK, benzene, hexenal + monoterp. and phenol. Their individual diurnal cycles are plotted in Appendix J, Figure J3. The diurnal patterns of acetone and MEK concentrations are very similar, with high levels during daytime. This probably refers to a third source being important for these two compounds (cf. Section 3.3). The Hexenal + monoterp. mass was characterized by a peak in the morning (centred at 9:00 UTC), but with a less pronounced diurnal cycle. Phenol showed a peak in the evening, wider than the wood burning peak. Several sources most likely contribute to this pattern. The diurnal cycle of propenal was defined by a peak in the evening that could be related either to wood burning or traffic and a small peak in the morning, maybe due to traffic. A non-negligible third source cannot be ruled out (cf. Section 3.3).

The four-parameters classification and the temporal variation study allowed to determine VOCs highly associated with wood burning (e.g. acetic acid, furfural) or traffic (e.g. toluene, C8-arom.); and other compounds with influences from both sources (benzene) or with lower or no association with these sources (acetone, MEK).

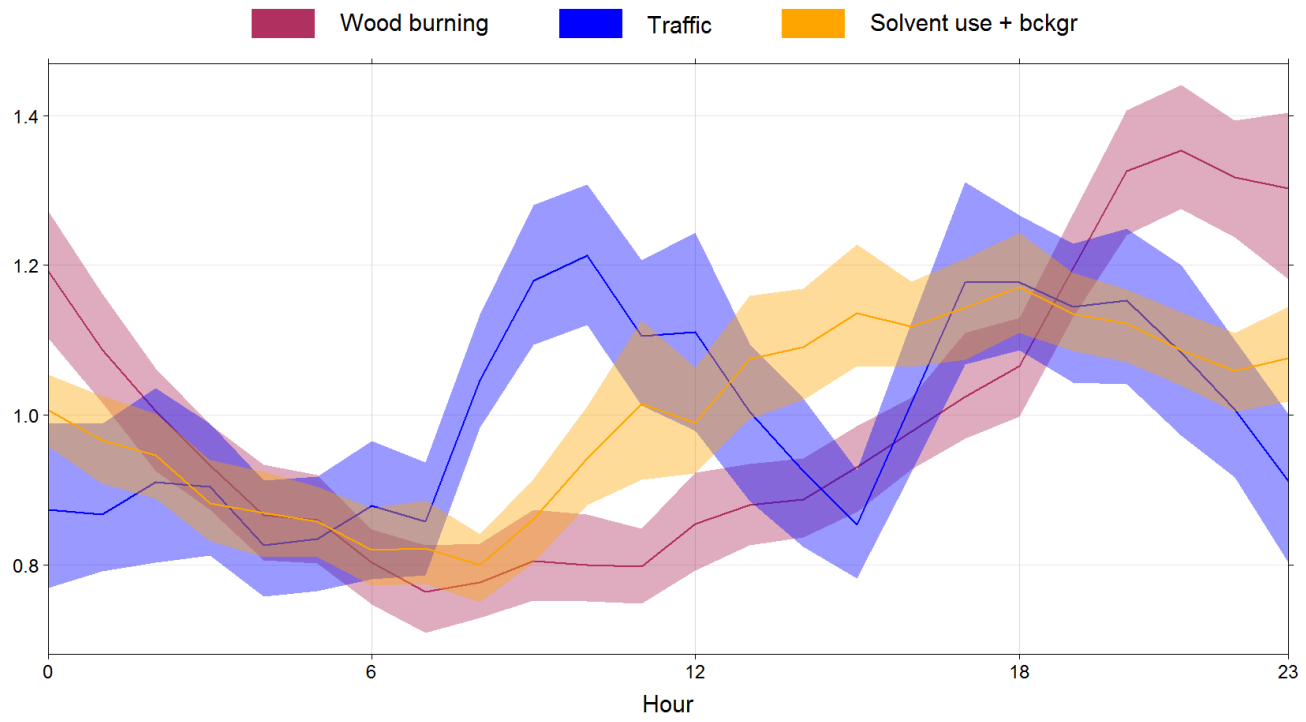

Figure 3 Diurnal cycle of the 3 PMF factors, identified as wood burning, traffic and solvent use + background (bckgr.).

3.3 VOC source apportionment at SIRTA using PMF

In addition to the qualitative analysis of wood burning and traffic sources (Section 3.2), PMF was computed to quantify the importance of these two sources as well as to investigate other possible sources.

3.3.1 Factors identification

BC fractions were used as independent tracers in order to evaluate the identification of the obtained PMF factor. The traffic-related and wood burning-related factors display typical diurnal cycles (Figure 3), confirmed by high correlations between the wood burning factor and BC_{wb} (r = 0.76) and between the traffic factor and $BC_{traffic}$ (r = 0.70), respectively. The third factor exhibits a diurnal cycle very close to the one found in a previous study in Paris (Baudic et al., 2016), attributed to solvent use. The chemical compositions present similarities, with an important contribution of acetone. The diurnal cycle of this third factor is flatter than the other ones, indicating a portion of background is included in this factor. However, adding a fourth factor did not lead to the separation of the solvent use from the background (see related discussion in Appendix C). Here, the third factor was then considered as solvent use plus background, even though a small amount of secondary compounds from chemical reactions cannot be ruled out. The present study being focused on wood burning and traffic, this third factor was not further investigated.

3.3.2 Wood burning and traffic composition and contributions

According to the PMF results (Figure 4), the wood burning source is dominant for 17 VOCs: furfural, acetic acid, methylbutenone, methylacetate, butandione, methylfuran, furan, propene+, furandione, benzenediol, benzene, formaldehyde,

methanol, chlorobenzene, phenol, butenal and hexenal + monoterp. All these VOCs were identified as wood burning influenced using the diurnal pattern study (except benzene and phenol) and most of them with the 4-parameters tool. In total, 12 VOCs were strongly associated with wood burning by all three methods (4-parameters tool, diurnal pattern study and PMF): methanol, propene+, acetic acid, furan, methylacetate, methylfuran, methylbutenone, butandione, furfural, furandione, benzenediol and chlorobenzene.

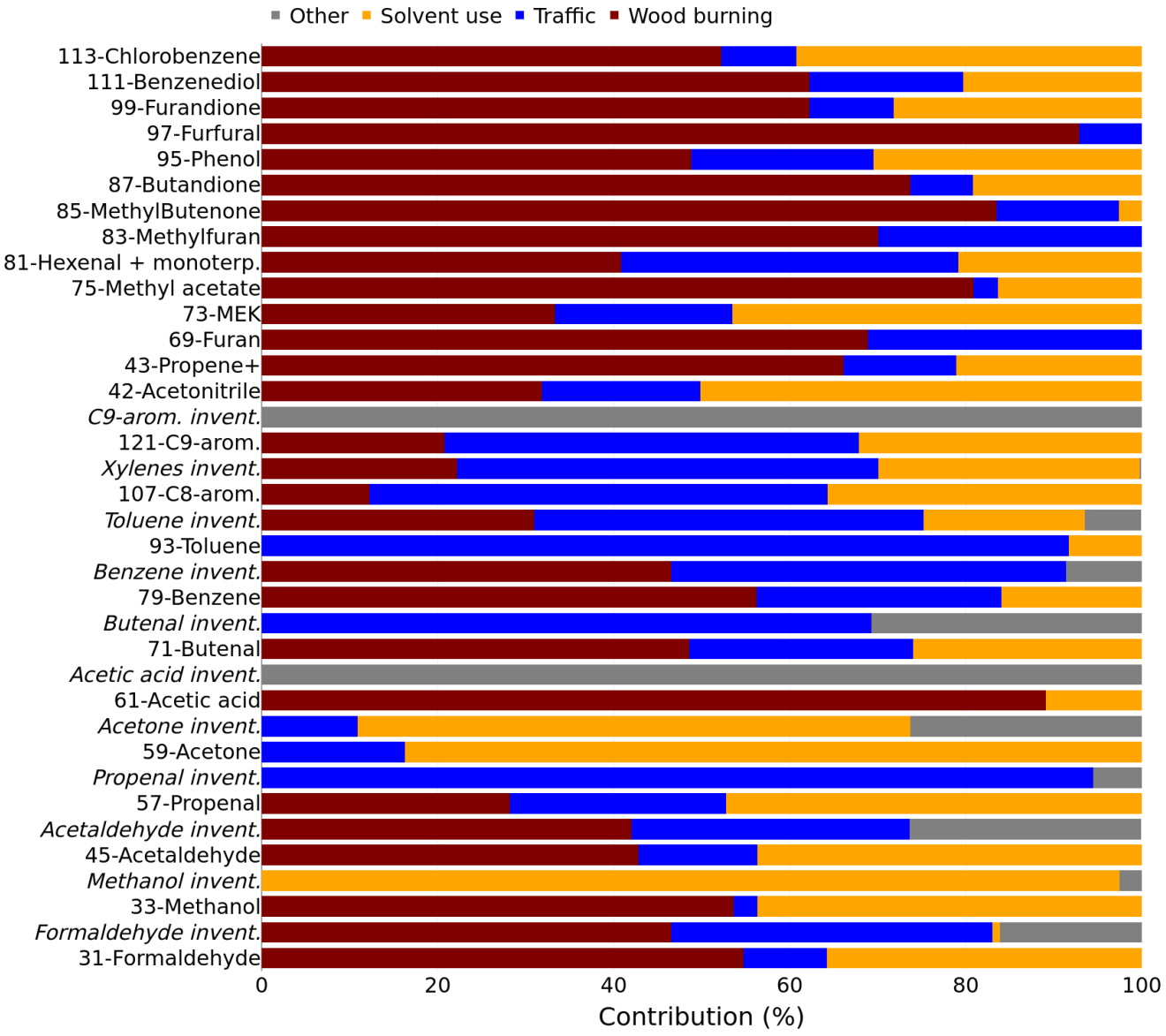

Figure 4 Factors contribution to each VOC (from the PMF results, VOCs names begin with the mass number), and sources contribution from the Airparif emission inventory to VOC also present in the database for PMF analysis (related labels are in italic and end with "invent." for the inventory). The bottom of the figure corresponds to compounds included both in the PMF analysis and in the inventory and the top to compounds only included in the PMF analysis.

Traffic was found to be the main source for three compounds: toluene, C8-arom. and C9-arom. They were already identified as traffic related by the 4-parameters tool as well as by the diurnal pattern analysis. The PMF results showed that traffic is

also responsible for a non-negligible part of hexenal + monoterp., furan (which can also be isoprene), methylfuran and benzene.

It is noteworthy that wood burning seemed to be responsible for a quite important fraction of a majority of VOCs. Except for toluene, C8-arom. and C9-arom. (traffic markers) and acetone (which was strongly associated with solvent use plus background), the wood burning contribution to each VOC exceeded 28 %. The traffic source dominates fewer compounds, i.e. toluene and C8- and C9-arom. The solvent use plus background source was primarily composed of acetone (most likely linked with solvent use) and few other compounds, such as acetonitrile, propenal and MEK.

3.3.3 Sources contributions and comparison with other studies

Wood burning was responsible for 47 % of the measured VOCs, traffic 22 % and solvent use plus background 31 % (Figure 5).

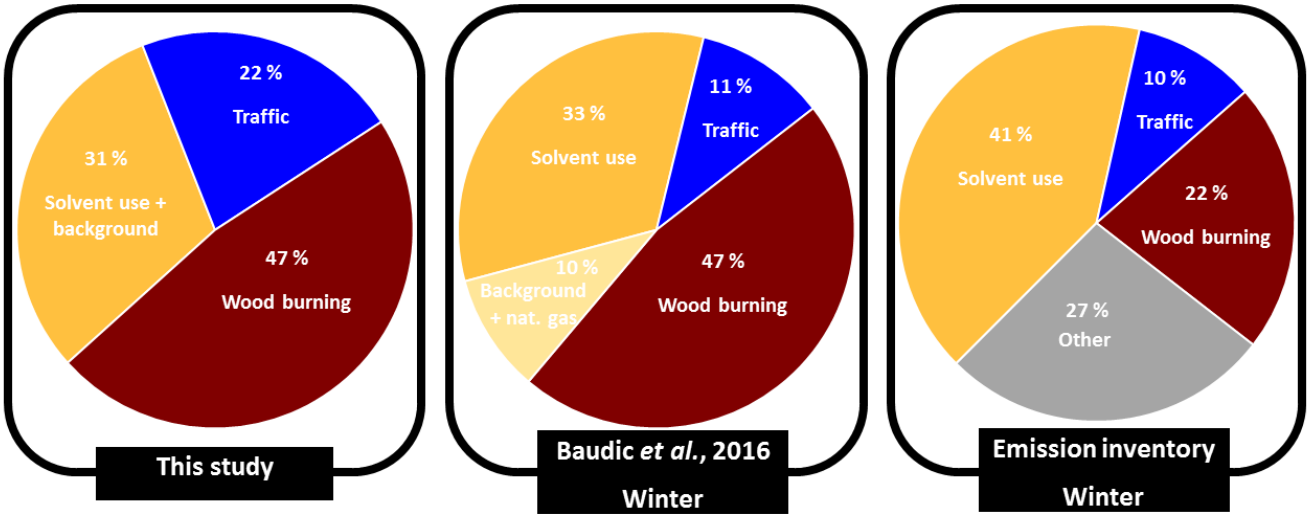

Figure 5 Sources contributions to the measured VOCs: comparison between the Baudic (2016) study, the emissions inventory from Airparif and this work.

Baudic et al. (2016) previously conducted a PMF analysis on VOC measurements in Paris, with a strikingly similar contribution from wood burning of 47 %. Although both studies are geographically and temporally separated, as well as based on different compounds, their consistency seems to underline the stability of the wood burning importance over the range of almost a decade. Also solvent use factors are generally similar between the two studies contributing to around a third of the measured VOCs. However, traffic was twice as important in the present work (22 % of the measured VOCs compared to 11 %), which might be partly due to the discrepancy in VOCs considered. The significance of the traffic source may be overestimated in the present study if parts of the background were misclassified.

3.3.3 Comparison between PMF outputs and the local emission inventory

Emission inventories are widely used as input data for chemical transport models, and hence for air quality forecasting and the assessment of public policies. However, uncertainties of these inventories are still high and some discrepancies with ambient measurements have been noticed recently (Gaimoz et al., 2011; Baudic, 2016). It is therefore of great importance to compare emission inventories with ambient measurements, notably allowing to check for their consistency. Two kinds of comparison between the PMF results and the local inventory (developed by Airparif) were conducted, as described hereafter.

First, a global comparison taking into account both all the VOCs available in the inventory and all the VOCs considered in the PMF. The predominant VOCs in the PMF were characterized by long lifetimes (e.g. methanol and acetone with lifetimes of about12 and 58 days, respectively, for an OH concentration of 10^6 molecules.cm^{-3}). This global comparison is therefore not expected to be substantially biased by any discrepancy between PMF factors and source fingerprints. Significant discrepancies exist between the inventory and the PMF results (Figure 5). The wood burning contribution seems to be particularly underestimated in the inventory. It reaches only 22 % of the emissions while almost half of the measured VOCs are attributed to wood burning both in the Baudic et al. (2016) and in the present study. The inventory attributes 10 % of the emissions to traffic, this is closer to the Baudic et al. (2016) results (11 %) than from our study (22 %). The solvent use-related emissions were estimated to represent a contribution of 41 %, which is slightly more than the results from the PMF studies. The inventory may slightly overestimate the solvent use emissions as suggested by previous studies (Gaimoz et al., 2011). According to the inventory, contributions from sources other than the three considered here are significant (27 %). The main sources gathered in this bin are industrial processes (except the solvent use in industry) and construction work, sources which were not identified in the present study. Light hydrocarbons were not measured. As for instance ethane and propane strongly drive the natural gas source, it was not identified here. Without considering the other sources in the inventory, the relative contributions of wood burning, traffic and solvent use would be 30 %, 14 % and 56 % respectively, i.e. wood burning would still be underestimated. This discrepancy could be explained by the fraction of non-measured VOCs in the three emission sectors considered here. Indeed, in the inventory, the contributions of VOCs considered in the PMF represent 13 % for wood burning, 34 % for traffic and 9 % for solvent use. Therefore, the VOCs considered in the PMF are only partially representative of the VOCs considered in the inventory but nevertheless the proportions for wood burning and solvent use are almost equivalent. We note that our results (47 % of the VOCs imputed to wood burning) are in agreement with Baudic et al. (2016), the latter including a larger part of the VOCs considered by the emission inventory. Hence, results confirm the wood burning source may be underestimated by the inventory.

The second kind of comparison with the inventory was conducted compound by compound, including eleven compounds: formaldehyde, methanol, acetaldehyde, propenal, acetone, acetic acid, butenal, benzene, toluene, xylenes (C8-arom. for the PMF dataset), and C9-aromatics. This selection represents 12 % of the total emissions in the inventory for winter (namely 2048 tons compared to 17802 tons). It is therefore not representative of the whole inventory (for instance, light hydrocarbons are not considered here) but a comparison based on these eleven VOCs is still relevant to suggest first explanations

concerning this underestimation of wood burning contributions by the inventory. The most reactive VOCs in this selection are trimethylbenzenes (part of the C9-aromatics). Their constant rates with OH span from 3.2 to $5.7.10^{-11}$ $cm^{-3}.molecule^{-1}.s^{-1}$ (Atkinson, 1990, 2000), leading to a lifetime of 2.5 hours at the shortest. For such highly reactive VOC, a bias can exist between the inventory (considering emissions) and the PMF study (based on observations). Figure 4 presents the source contribution (wood burning, traffic, solvent use and other sources) for these VOCs. Xylenes present excellent similarities for the three sources. Very close results appeared for benzene, both for wood burning and traffic influence. Satisfactory consistency was found for formaldehyde and acetaldehyde, especially for the wood burning apportionment. Acetone is also found to be mainly of solvent use origin by both methods. However, discrepancies were also encountered. Methanol emissions are almost exclusively attributed to solvent use in the inventory, despite a significant wood burning influence identified here. Considering the long lifetime of this VOC (more than 10 days), this difference cannot be induced by chemical reactions between emission and measurement. Propenal and butenal emissions were considered to be mostly from traffic while this study showed other influences (wood burning and solvent use). On the contrary, the inventory considered toluene to be emitted by wood burning and solvent use for a non-negligible part whereas the PMF concluded traffic emissions contribute 92 % to this pollutant. This strong association between toluene and traffic was underlined in previous studies, especially in a tunnel experiment where the traffic source was extensively studied (Ammoura et al., 2014; Baudic et al., 2016). To conclude, results presented here indicate that some entries in the Airparif emission inventory should be adjusted. According to the inventory, acetic acid and C9-arom. are emitted by only one source each, namely beer brewing and locomotives, respectively. This clearly contradicts the major influences of wood burning and traffic identified here. The atmospheric lifetime of acetic acid is about 2-4 days, which is long enough to exclude the chemistry as an explanation for the discrepancy between the inventory and the PMF results. As mentioned before, C9 arom. are characterized by a short lifetime. However, its strong association with traffic confirms that corrections should be implemented in the inventory concerning this compound.

To conclude the comparison between the PMF results and the Airparif inventory, good consistency was found for some compounds while significant discrepancies were identified for others. Particularly, the wood burning source in the inventory seemed to be globally under-estimated. Uncertainties related to this source in the inventory are difficult to assess. They are mostly linked to the amount and spatial distribution of wood burning activities, the emission factors of burning appliances and their burning efficiency. The discrepancy between our PMF results and the inventory concerning wood burning can be partly explained by inaccurate source attribution for a certain VOC in the inventory (e.g. acetic acid, methanol). Some VOCs emitted by wood burning are important SOA precursors (e.g. phenol, benzenediol) but they are not considered in the inventory. These shortcomings lead to uncertainties in chemical models. As wood burning is a major VOC emitter during winter, an updated inventory would improve model results, likely enabling refined forecasting of winter pollution episodes in the Paris region.

3.4 Spatial variabilities

Measurements conducted at several locations (Appendix A, Figure A1) allowed for the investigation of spatial variations across the Île-de-France region.

3.4.1 NO_x and BC site-to-site comparison

SIRTA was characterized by low NO over NO_2 ratio (0.27 ppb.ppb^{-1}), compared to traffic stations (between 1.4 and 3.4 ppb.ppb^{-1}) and even to urban stations (0.50 and 0.43 ppb.ppb^{-1}). This station typology is confirmed again by BC, $BC_{traffic}$, NO and NO_2 levels, which are much higher at the traffic stations compared to SIRTA (results are presented in details in Appendix K, Figure K1).

Considering BC_{wb}, the differences between the site locations were smaller but with the same ranking order: the largest concentrations were measured at the urban Airparif stations, Gennevilliers and Paris XIII^e. The median of BC_{wb} was 321 ng.m^{-3} for the Paris XIII^e station while the LISA and SIRTA stations had the lowest values (medians of 115 and 143 ng.m^{-3}, respectively). Furthermore, correlations between the stations (Appendix L, Figure L1) highlight pollutants vary rather simultaneously and concentrations over the region were more homogeneous for wood burning sources, as correlation coefficients of BC_{wb} (0.73 on average) clearly exceeded those of $BC_{traffic}$ (0.39 on average).

3.4.2 VOC site-to-site comparison

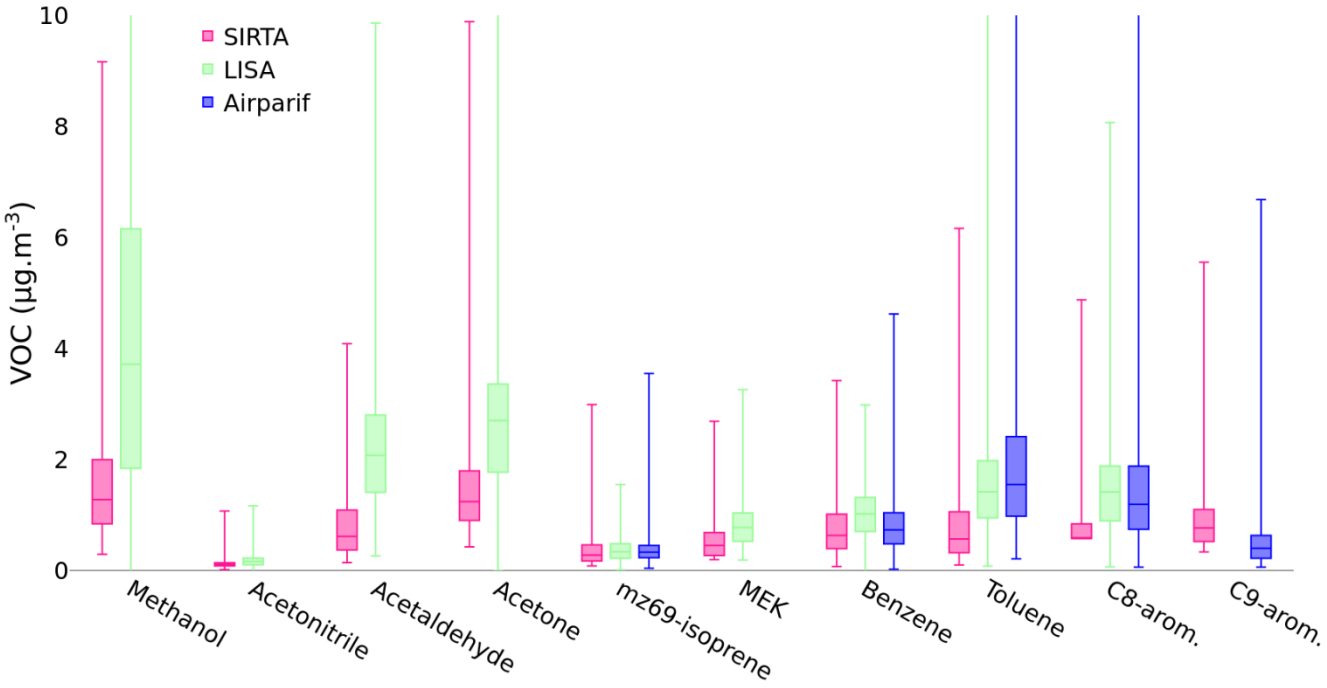

Figure 6 Box plot for VOCs measurements from the three VOCs stations: SIRTA, LISA and Airparif. The measured compounds called "mz69-isoprene" refer to isoprene for Airparif and to the PTR-MS mass 69 for the SIRTA and LISA stations. For Airparif, "C8-arom." refer to isoprene for Airparif and to the PTR-MS mass 69 for the SIRTA and LISA stations. For Airparif, "C8-arom." refers to the sum of m-p-xylenes, o-xylene and ethylbenzene; and "C9-arom." refers to the sum of 1,3,5trimethylbenzene,

1,2,3trimethylbenzene and 1,2,4trimethylbenzene. The box represents the upper and lower quartiles and the whiskers reach extreme values. The picture was reframed for a better readability. Due to blank problems, considered methanol values from LISA are restricted to the period 2 – 12 February 2018. The whole dataset was considered for SIRTA, the related period (Nov. 2017 – March 2018) was extracted from the long-term Airparif measurements and data from LISA is available for the shorter period (February – March 2018 as detailed in Section 2.2).

Figure 6 shows the distributions of VOCs monitored at all three sites. For all VOCs, concentrations at LISA were higher than at SIRTA, with most pronounced increments for methanol, acetaldehyde and acetone. Concentrations of C9-arom. were lower at the dense urban Airparif site compared to at SIRTA, which is likely explained by measurement uncertainty induced by the poor selectivity of the measurement technique applied at SIRTA (Section 2.1.2). For the SIRTA observations, the group of C9-arom. includes several additional compounds such as methylbenzaldehyde and phenylethanone. m/z 69-isoprene observations, agree extremely well between the three sites. The diurnal cycle of isoprene (selective measurement) from Airparif (not shown) suggests a fraction of anthropogenic emission for this compound. It is therefore possible that a balanced mix of isoprene and furan was monitored by PTR-MS at m/z 69. Benzene concentrations at the three stations were also very similar, which is presumably explained by its long lifetime of several days. Toluene and C8-arom. (defined by shorter lifetimes) have similar levels at the LISA and Airparif stations, but clearly lower concentrations at SIRTA.

While overall concentrations enable general characterization of the stations' typology, correlations between observations at the three sites provides information about the relative variability encountered in the different environments. The correlations between VOCs are summarised in a correlation matrix (Appendix M, Figure M1). For toluene, the correlations including observations at SIRTA were low (0.39 with Airparif and 0.48 with LISA), while the correlation was stronger between Airparif and LISA (0.62). For benzene, correlations were generally higher ($r_{Airparif\text{-}SIRTA}$ = 0.67, $r_{Airparif\text{-}LISA}$ = 0.70 and $r_{LISA\text{-}SIRTA}$ = 0.57). For other VOCs related to wood burning such as methanol and acetaldehyde, correlations between the SIRTA and LISA observations were strong (0.74 and 0.67). The lifetime of the compound impacts the correlation of its concentration observed simultaneously at two contrasting locations. However, this effect alone would not explain the discrepancies found here as acetaldehyde is characterized by a shorter lifetime than toluene and yet the correlation (between SIRTA and LISA) was stronger for acetaldehyde than for toluene.

The benzene over toluene ratio is widely used as an indicator of traffic or wood burning influences. At LISA, it reached 0.73 $ppb.ppb^{-1}$ and at Airparif, the benzene over toluene ratio was on average 0.59 $ppb.ppb^{-1}$. This is a typical value for a dense urban place strongly influenced by traffic. Gaeggeler et al. (2008) found a value between 0.51 and 0.54 $ppb.ppb^{-1}$ for Zürich city centre. At SIRTA, this ratio was as high as 1.84 $ppb.ppb^{-1}$. Which is much more than the benzene over toluene ratio measured by Gaeggeler et al. (2008) in the Roveredo village, where both wood burning and traffic sources were important. The ratio at SIRTA is closer to those reported for wood stove emissions (Sällsten et al., 2006; Hedberg et al., 2002) (1.7 and between 1.4 and 5 $ppb.ppb^{-1}$ respectively). This enables to conclude that wood burning has, in relation to the

other studied sources, a stronger impact at SIRTA while traffic has a stronger impact at the Airparif and LISA stations. Similar levels and higher correlations were found between the stations for wood burning-related compounds (see discussion on methanol and acetaldehyde), whereas levels of traffic-associated pollutants clearly differ between locations and correlations are poorer.

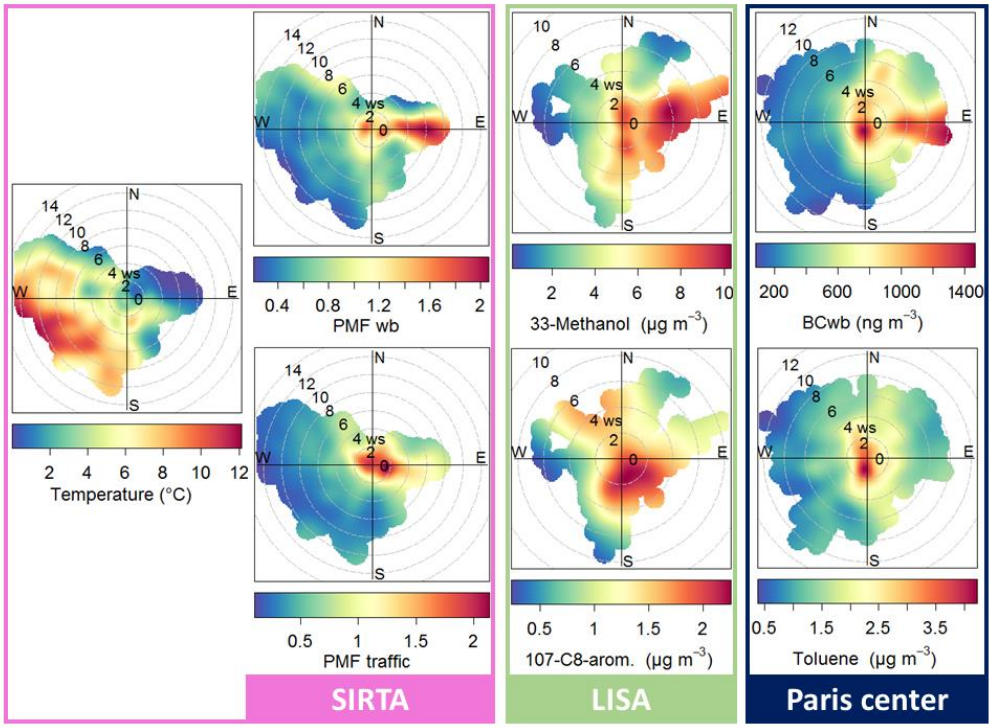

Figure 7 Polar plot of the temperature and a selection of compound and PMF factor concentrations as a function of wind (speed and direction) at SIRTA, LISA (Creteil) and Paris city centre (Airparif head office for toluene and Haussmann station for BC_{wb}).

3.4.3 Association with wind and temperature

For a selection of compounds, the influence of wind speed and direction on concentrations was assessed at the SIRTA, LISA and Airparif stations (Figure 7). Two different patterns arose: a wood burning-related pattern (on the first row) represented by the PMF output, methanol and BC_{wb} and a traffic-related pattern (on the second row) represented by the PMF output, C8-arom. and toluene. Similar results were obtained for other compounds associated either with wood burning or traffic (Appendix N).

The traffic pattern showed strongest concentrations for a slow wind speed (below 2 m.s^{-1}) with no particular wind direction. Even if results were less clear at LISA, the traffic pattern is consistent between compounds. This highlighted that the highest levels of traffic-related pollution were most likely induced by stagnant meteorological conditions, when the dispersion is weak. Traffic pollutants are therefore mainly of local origin.

Concerning the wood burning pattern, highest concentrations were associated with easterly winds at a speed ranging between 4 and 8 $m.s^{-1}$. However, it is important to note that the lowest temperatures were also associated with these wind directions (Figure 7), suggesting a prevalent influence of meteorological conditions (rather than air mass origins) onto wood burning pollutant concentrations, which could be partly due to more intense residential heating emissions.

4 Discussion and conclusion

The main goals of this study were to investigate (i) the qualitative identification of wood burning and traffic influences on VOC ambient concentrations, (ii) the quantification of the source contribution, notably allowing the comparison with the emission inventory and (iii) the characterisation of the spatial variability of the considered pollutants over the Paris region.

The first result of this study was the identification of VOCs associated with wood burning and traffic sources. Three methods enabled this identification: a 4-parameters classification, a diurnal cycle study and PMF apportionment. The combination of the three methods identified 12 VOCs were strongly associated with wood burning emissions (methanol, propene+, acetic acid, furan, methylacetate, methylfuran, methylbutenone, butandione, furfural, furandione, benzenediol and chlorobenzene), while three VOCs were clearly related to traffic (toluene, C8-arom. and C9-arom.) In addition, two VOCs were predominantly linked to solvent use (acetone and MEK).

Of the 17 wood burning-related VOCs identified by Gaeggeler et al. (2008) six compounds were also closely related to this source by the present study (propene+, methylacetate, methanol, furandione, acetic acid and propanol), while others (acetaldehyde, acetone and propanal, butanal and MEK, propenal, MVK and methacrolein) also had significant contributions from other sources. For instance, acetaldehyde was also imputed to solvent use in our study, in agreement with Baudic et al. (2016). The Gaeggeler et al. (2008) study was conducted in a small Alpine valley with a weak influence of sources other than wood burning and traffic, which could explain the discrepancy. The difference in signature for propenal, butanal and MEK could also be explained by an important influence of solvent use in the Paris region. Coggon et al. (2016) found methylfuran and furfural as wood burning tracers, and temper the classification of acetonitrile as a relevant wood burning tracer, as it was often considered before (Holzinger et al., 1999). This is consistent conclusions drawn here: methylfuran and furfural were closely related to wood burning while solvent use was imputed to be the major acetonitrile emitter. Further, results agree with Bruns et al. (2016) identifying furan, methylbutenone, butandione and benzenediol as predominantly emitted by wood burning activities. Surprisingly, we did not measure any clear signal for naphthalene despite of its previous use as tracer (Bruns et al., 2016; Baudic, 2016). This may be due to losses along the line for larger masses in present experiment. Phenol, with significant emissions registered by Bruns et al. (2017), was not measured clearly here, which could be explained by the short lifetime of this VOC (around 7 hours for [OH] = 1.6 10^6 molecules cm^{-3}). Chlorobenzene was here strongly associated with wood burning although this was not commonly concluded elsewhere, only Nádudvari et al. (2018) related this compound with coal combustion. For the first time (to the best of our knowledge), methylbutenone, benzenediol and butandione were identified as wood burning related in ambient air. Benzene is an important VOC, often monitored

mostly because of its impact on health. It is emitted by several sources. According to the PMF results presented, it is explained mostly by wood burning (56 %) but with an important traffic contribution (28 %). This is in agreement with Hellén et al. (2008) and Panopoulou et al. (2018) who identified both traffic and wood burning as main benzene emitters. Regarding the traffic associated VOCs, Gaeggeler et al. (2008) identified xylenes and trimethylbenzene. We had a similar result with the m/z 107 and 121, identified as C8-arom. and C9-arom. However, Gaeggeler et al. (2008) did not associate toluene with traffic while the PMF results showed a traffic origin of 92 %. Toluene was already identified as a major traffic emitted VOC in tunnel studies, in particular in a tunnel near Paris (Ammoura et al., 2014; Baudic et al., 2016). Like in the present study, acetone has before been reported to be largely due to solvent use (Gaimoz et al., 2011, Baudic et al., 2016).

Among the three methods used in order to associate VOCs to whether traffic or wood burning source origin, the 4-parameters method was found to have some advantages: it is an efficient tool with quantitative parameters easily conducted systematically. The main drawback is that it is less efficient for VOCs influenced by other sources than traffic and wood burning. Studying the diurnal cycles is valuable to point out VOCs emitted by two sources or more, however it is a subjective and qualitative procedure. The PMF computations linked the preponderant VOCs to each source. This is a quantitative tool, but requiring complex and time-demanding settings to achieve robust results.

The PMF quantitative source apportionment assigned 47 % of the measured VOCs to wood burning and 22 % to traffic. These results are close to those by Baudic et al. (2016), especially for the wood burning source. Knowing that different VOCs were considered in the two studies, this consistency demonstrates that in these conditions (in winter in Île-de-France), wood burning is the predominant VOC source, representing about half of the total concentrations (both if the major considered compounds are light hydrocarbons or oxygenated VOCs). PMF was also used for a comparison to the regional emissions inventory. Significant discrepancies were found for wood burning (22 % of the total VOCs in the inventory *versus* 47 % in our study) and for traffic (10 % of the total VOCs in the inventory *versus* 22 % in our study). These differences may be explained by an erroneous attribution for some VOCs by the inventory. Even if good consistency was found for some compounds such as benzene and xylenes, results suggest improvements could be implemented for several other VOCs (especially acetic acid, C9-arom. and methanol).

As traffic pollution was highly variable over the region (with highest concentrations monitored in dense urban places) and strongest levels were measured during stagnant meteorological conditions with a low wind speed, it was concluded that traffic sources are of predominantly local origin, confirming previous studies (e.g., Panopoulou et al., 2018). Wood burning-related pollutants were found to be more homogeneous over the region and mainly driven by meteorological conditions (wind and air temperature).

The present study contains some limitations. The wood burning identification was mostly based on temporal variabilities (using several methods); and even if independent tracers (BC_{wb} and levoglucosan) were used to strengthen the identification, it cannot absolutely be ruled out that other VOC heating sources (gas, heating oil, coal, etc.) with a similar temporal variation

are partly misclassified as wood burning. This may result in a small over-estimation of the wood burning impact on pollution. Further investigations considering specific gas tracers could quantify this potential over-estimation. In addition, the quadrupole used as detector in this study did not allow differentiating compounds having the same unitary mass. A PTR-ToF-MS instrument would enable both a better mass resolution and the quantification of heavier masses with a shorter time step. This would be useful to further investigate in ambient air the VOCs identified by Bruns et al. (2016, 2017).

Several perspectives can be highlighted to follow from this study. First, the solvent use factor needs to be analysed in more detail, both to separate the background contribution and to understand better this important source (31 % of the measured VOCs). Secondly, SOA formation partly remains an open question. Some VOCs previously characterized as main SOA precursors (Bruns et al., 2016), such as phenol, benzene, benzenediol and methylfuran were measured in ambient air. However, heavier compounds such as polycyclic aromatic hydrocarbons need to be further examined in ambient air (Nalin et al., 2016). Further studies, notably including aerosol mass spectrometry, could improve the understanding of wood burning and traffic impact on SOA formation.

References

ACTRIS, Final SOPs for VOCs measurements, Version 2014/09/30, http://www.actris.eu/Portals/46/Data%20and%20Services/Measurement%20guidelines/Near-surface%20trace%20gases/ACTRIS-1%20Deliverable_WP4_D4.9_M42_v2_Sep2014.pdf?ver=2017-03-20-135044, 2014.

Airparif: Bilan des émissions atmosphériques en Île-de-France, Année de référence 2015, Airparif, pp. 1–87, 2019.

Ait-Helal, W., Borbon, A., Sauvage, S., de Gouw, J. A., Colomb, A., Gros, V., Freutel, F., Crippa, M., Afif, C., Baltensperger, U., Beekmann, M., Doussin, J.-F., Durand-Jolibois, R., Fronval, I., Grand, N., Leonardis, T., Lopez, M., Michoud, V., Miet, K., Perrier, S., Prévôt, A. S. H., Schneider, J., Siour, G., Zapf, P., and Locoge, N.: Volatile and intermediate volatility organic compounds in suburban Paris: variability, origin and importance for SOA formation, Atmospheric Chemistry and Physics, 14, 10439–10464, https://doi.org/10.5194/acp-14-104392014, https://www.atmos-chem-phys.net/14/10439/2014/, 2014.

Ammoura, L., Xueref-Remy, I., Gros, V., Baudic, A., Bonsang, B., Petit, J.-E., Perrussel, O., Bonnaire, N., Sciare, J., and Chevallier, F.: Atmospheric measurements of ratios between CO2 and co-emitted species from traffic: a tunnel study in the Paris megacity, Atmospheric Chemistry and Physics, 14, 12871–12882, https://doi.org/10.5194/acp-14-12871-2014, https://www.atmos-chem-phys.net/14/12871/2014/, 2014.

Atkinson, R.: Gas-phase Tropospheric Chemistry of Organic Compounds: A review, Atmospheric Environment. Part A. General Topics, 24, 1–41, https://doi.org/10.1016/0960-1686(90)90438-S, 1990.

Atkinson, R.: Atmospheric chemistry of VOCs and NOx. Atmos. Environ. 34:2063-2101, Atmospheric Environment, 34, 2063–2101, 15 https://doi.org/10.1016/S1352-2310(99)00460-4, 2000.

Baasandorj, M., Millet, D. B., Hu, L., Mitroo, D., and Williams, B. J.: Measuring acetic and formic acid by proton-transfer-reaction mass spectrometry: sensitivity, humidity dependence, and quantifying interferences, Atmospheric Measurement Techniques, 8, 1303–1321, https://doi.org/10.5194/amt-8-1303-2015, https://www.atmos-meas-tech.net/8/1303/2015/, 2015.

Bari, M. A. and Kindzierski, W. B.: Ambient volatile organic compounds (VOCs) in Calgary, Alberta: Sources and screening health risk assessment, Science of The Total Environment, 631-632, 627 – 640, https://doi.org/https://doi.org/10.1016/j.scitotenv.2018.03.023, http://www.sciencedirect.com/science/article/pii/S0048969718307782, 2018.

Barrefors, G. and Petersson, G.: Volatile hydrocarbons from domestic wood burning, Chemosphere, 30, 1551 – 1556, https://doi.org/https://doi.org/10.1016/0045-6535(95)00048-D, http://www.sciencedirect.com/science/article/pii/004565359500048D, 1995a.

Barrefors, G. and Petersson, G.: Assessment by gas chromatography and gas chromatography-mass spectrometry of volatile hydrocarbons from biomass burning, Journal of Chromatography A, 710, 71 – 77, https://doi.org/https://doi.org/10.1016/0021-9673(95)000025, http://www.sciencedirect.com/science/article/pii/0021967395000025, chromatography and Electrophoresis in Environmental Analysis: Air Pollution, 1995b.

Baudic, A.: Caractérisation expérimentale et statistique des sources de Composés Organiques Volatils (COV) en région Île-de-France, Ph.D. thesis, http://www.theses.fr/2016SACLS537, thèse de doctorat dirigée par Gros, Valérie et Bonsang, Bernard Météorologie, océanographie, physique de l'environnement Paris Saclay 2016, 2016.

Baudic, A., Gros, V., Sauvage, S., Locoge, N., Sanchez, O., Sarda-Estève, R., Kalogridis, C., Petit, J.-E., Bonnaire, N., Baisnée, D., Favez, O., Albinet, A., Sciare, J., and Bonsang, B.: Seasonal variability and source apportionment of volatile organic compounds (VOCs) in the Paris megacity (France), Atmospheric Chemistry and Physics, 16, 11961–11989, https://doi.org/10.5194/acp-16-11961-2016, http: 35 //www.atmos-chem-phys.net/16/11961/2016/, 2016.

Beekmann, M., Prévôt, A. S. H., Drewnick, F., Sciare, J., Pandis, S. N., Denier van der Gon, H. A. C., Crippa, M., Freutel, F., Poulain, L., Ghersi, V., Rodriguez, E., Beirle, S., Zotter, P., von der Weiden-Reinmüller, S.-L., Bressi, M., Fountoukis, C., Petetin, H., Szidat, S., Schneider, J., Rosso, A., El Haddad, I., Megaritis, A., Zhang, Q. J., Michoud, V., Slowik, J. G., Moukhtar, S., Kolmonen, P., Stohl, A., Eckhardt, S., Borbon, A., Gros, V., Marchand, N., Jaffrezo, J. L., Schwarzenboeck, A., Colomb, A., Wiedensohler, A., Borrmann, S., Lawrence, M., Baklanov, A., and Baltensperger, U.: In situ, satellite measurement and model evidence on the dominant regional contribution to fine particulate matter levels in the Paris megacity, Atmos. Chem. Phys., 15, 9577-9591, https://doi.org/10.5194/acp-15-9577-2015, 2015.

Blake, R. S., Monks, P. S., and Ellis, A. M.: Proton-Transfer Reaction Mass Spectrometry, Chemical Reviews, 109, 861–896, https://doi.org/10.1021/cr800364q, https://doi.org/10.1021/cr800364q, pMID: 19215144, 2009.

Bressi, M., Sciare, J., Ghersi, V., Mihalopoulos, N., Petit, J.-E., Nicolas, J. B., Moukhtar, S., Rosso, A., Féron, A., Bonnaire, N., Poulakis, E., and Theodosi, C.: Sources and geographical origins of fine aerosols in Paris (France), Atmospheric Chemistry and Physics, 14, 8813–8839, https://doi.org/10.5194/acp-14-8813-2014, https://www.atmos-chem-phys.net/14/8813/2014/, 2014.

Bruns, E., El Haddad, I., G. Slowik, J., Kilic, D., Klein, F., Baltensperger, U., and Prevot, A.: Identification of significant precursor gases of secondary organic aerosols from residential wood combustion, 6, 27881, 2016.

Bruns, E. A., Slowik, J. G., El Haddad, I., Kilic, D., Klein, F., Dommen, J., Temime-Roussel, B., Marchand, N., Baltensperger, U., and Prévôt, A. S. H.: Characterization of gas-phase organics using proton transfer reaction time-of-flight mass spectrometry: fresh and aged residential wood combustion emissions, Atmospheric Chemistry and

Physics, 17, 705–720, https://doi.org/10.5194/acp-17-705-2017, https://www.atmos-chem-phys.net/17/705/2017/, 2017.

Buzcu-Guven, B. and Fraser, M. P.: Comparison of VOC emissions inventory data with source apportionment results for Houston, TX, Atmospheric Environment, 42, 5032 – 5043, https://doi.org/https://doi.org/10.1016/j.atmosenv.2008.02.025, http://www.sciencedirect.com/science/article/pii/S1352231008001805, 2008.

Carslaw D. C.and Ropkins K.: openair an R package for air quality data analysis. Environmental Modelling & Software, 27-28 :52 - 61, 2012.

Coggon, M. M., Veres, P., Yuan, B., Koss, A., Warneke, C., Gilman, J., Lerner, B., Peischl, J., Aikin, K., Stockwell, C., Hatch, L., Ryerson, T., Roberts, J., Yokelson, R., and Gouw, J.: Emissions of nitrogen-containing organic compounds from the burning of herbaceous and arboraceous biomass: Fuel composition dependence and the variability of commonly used nitrile tracers, geographical researche letters, 43, 9903–9912, https://doi.org/10.1002/2016GL070562, 2016.

Crippa, M., DeCarlo, P. F., Slowik, J. G., Mohr, C., Heringa, M. F., Chirico, R., Poulain, L., Freutel, F., Sciare, J., Cozic, J., Di Marco, C. F., Elsasser, M., Nicolas, J. B., Marchand, N., Abidi, E., Wiedensohler, A., Drewnick, F., Schneider, J., Borrmann, S., Nemitz, E., Zimmermann, R., Jaffrezo, J.-L., Prévôt, A. S. H., and Baltensperger, U.: Wintertime aerosol chemical composition and source apportionment of the organic fraction in the metropolitan area of Paris, Atmospheric Chemistry and Physics, 13, 961–981, https://doi.org/10.5194/acp-13961-2013, https://www.atmos-chem-phys.net/13/961/2013/, 2013.

de Gouw, J. and Warneke, C.: Measurements of volatile organic compounds in the earth's atmosphere using proton-transfer-reaction mass spectrometry, Mass Spectrometry Reviews, 26, 223–257, 2007.

Debevec, C., Sauvage, S., Gros, V., Sciare, J., Pikridas, M., Stavroulas, I., Salameh, T., Leonardis, T., Gaudion, V., Depelchin, L., Fronval, I., Sarda-Esteve, R., Baisnée, D., Bonsang, B., Savvides, C., Vrekoussis, M., and Locoge, N.: Origin and variability in volatile organic compounds observed at an Eastern Mediterranean background site (Cyprus), Atmospheric Chemistry and Physics, 17, 11355–11388, https://doi.org/10.5194/acp-17-11355-2017, https://www.atmos-chem-phys.net/17/11355/2017/, 2017.

Drinovec, L., Mo£nik, D., Zotter, P., Prévôt, A. S. H., Ruckstuhl, C., Coz, E., Rupakheti, M., Sciare, J., Müller, T., Wiedensohler, A., and Hansen, A. D. A. The "dual-spot" aethalometer: an improved measurement of aerosol black carbon with real-time loading compensation. Atmospheric Measurement Techniques, 8(5) :1965-1979, 2015.

EMEP, Transboundary particulate matter,photo-oxidants, acidifying and eutrophyingcomponents, https://emep.int/publ/reports/2016/EMEP_Status_Report_1_2016.pdf, 2016.

Evtyugina, M., Alves, C., Calvo, A., Nunes, T., Tarelho, L., Duarte, M., Prozil, S. O., Evtuguin, D. V., and Pio, C.: VOC emissions from residential combustion of Southern and mid-European woods, Atmospheric Environment, 83, 90 – 98, https://doi.org/https://doi.org/10.1016/j.atmosenv.2013.10.050, http://www.sciencedirect.com/science/article/pii/S1352231013008030, 2014.

Favez, O., Cachier, H., Sciare, J., and Le Moullec, Y.: Chararcterization and contribution to $PM_{2.5}$ of semi-volatile aerosols in Paris (France), Atmospheric Environment, 41, 7969-7976, doi: 10.1016/j.atmosenv.2007.09.031

Favez, O., Cachier, H., Sciare, J., Sarda-Estève, R., and Martinon, L.: Evidence for a significant contribution of wood burning aerosols to PM2.5 during the winter season in Paris, France, Atmospheric Environment, 43, 3640 – 3644, https://doi.org/https://doi.org/10.1016/j.atmosenv.2009.04.035, http://www.sciencedirect.com/science/article/pii/S1352231009003690, 2009.

Favez, O. and Amodeo, T.: ÉPISODES DE POLLUTION PARTICULAIRE DE DÉBUT DÉCEMBRE 2016, LCSQA, pp. 1–9, 2016.

Fourtziou, L., Liakakou, E., Stavroulas, I., Theodosi, C., Zarmpas, P., Psiloglou, B., Sciare, J., Maggos, T., Bairachtari, K., Bougiatioti, A., Gerasopoulos, E., Sarda-Estève, R., Bonnaire, N., and Mihalopoulos, N.: Multi-tracer approach to characterize domestic wood burning in Athens (Greece) during wintertime, Atmospheric Environment, 148, 89 – 101, https://doi.org/https://doi.org/10.1016/j.atmosenv.2016.10.011, http://www.sciencedirect.com/science/article/pii/S1352231016308081, 2017.

Freutel, F., Schneider, J., Drewnick, F., von der Weiden-Reinmüller, S.-L., Crippa, M., Prévôt, A. S. H., Baltensperger, U., Poulain, L., Wiedensohler, A., Sciare, J., Sarda-Estève, R., Burkhart, J. F., Eckhardt, S., Stohl, A., Gros, V., Colomb, A., Michoud, V., Doussin, J. F., Borbon, A., Haeffelin, M., Morille, Y., Beekmann, M., and Borrmann, S.: Aerosol particle measurements at three stationary sites in the megacity of Paris during summer 2009: meteorology and air mass origin dominate aerosol particle composition and size distribution, Atmos. Chem. Phys., 13, 933-959, https://doi.org/10.5194/acp-13-933-2013, 2013.

Gaeggeler, K., Prevot, A. S., Dommen, J., Legreid, G., Reimann, S., and Baltensperger, U.: Residential wood burning in an Alpine valley as a source for oxygenated volatile organic compounds, hydrocarbons and organic acids, Atmospheric Environment, 42, 8278 – 8287, https://doi.org/https://doi.org/10.1016/j.atmosenv.2008.07.038, http://www.sciencedirect.com/science/article/pii/ S1352231008006778, 2008.

Gaimoz, C., Sauvage, S., Gros, V., Herrmann, F., Williams, J., Locoge, N., Perrussel, O., Bonsang, B., d'Argouges, O., Sarda-Esteve, R., and Sciare, J.: Volatile organic compounds sources in Paris in spring 2007. Part II: source apportionment using positive matrix factorisation, Environmental chemistry, 8, 91–103, 2011.

Gros, V., Gaimoz, C., Herrmann, F., Custer, T., Williams, J., Bonsang, B., Sauvage, S., Locoge, N., d'Argouges, O., Sarda-Esteve, R., and Sciare, J.: Volatile organic compounds sources in Paris in spring 2007. Part I: qualitative analysis, Environmental chemistry, 8, 74–90, 2011.

Haeffelin, M., Barthès, L., Bock, O., Boitel, C., Bony, S., Bouniol, D., Chepfer, H., Chiriaco, M., Cuesta, J., Delanoë, J., Drobinski, P., Dufresne, J.-L., Flamant, C., Grall, M., Hodzic, A., Hourdin, F., Lapouge, F., Lemaître, Y., Mathieu, A., Morille, Y., Naud, C., Noël, V., O'Hirok, W., Pelon, J., Pietras, C., Protat, A., Romand, B., Scialom, G., and Vautard, R.: SIRTA, a ground-based atmospheric observatory for cloud and aerosol research, Annales Geophysicae, 23, 253–275, https://doi.org/10.5194/angeo-23-253-2005, https://www.ann-geophys.net/23/253/2005/, 2005.

Hazan, L., Tarniewicz, J., Ramonet, M., Laurent, O., and Abbaris, A.: Automatic processing of atmospheric CO2 and CH4 mole fractions at the ICOS Atmosphere Thematic Centre, Atmospheric Measurement Techniques, 9, 4719–4736, https://doi.org/10.5194/amt-9-4719-2016, https://www.atmos-meas-tech.net/9/4719/2016/, 2016.

Hedberg, E., Kristensson, A., Ohlsson, M., Johansson, C., Johansson, P., Swietlicki, E., Vesely, V., Wideqvist, U., and Westerholm, R.: Chemical and physical characterization of emissions from birch wood combustion in a wood stove, Atmospheric Environment, 36, 4823– 4837, https://doi.org/10.1016/S1352-2310(02)00417-X, the information about affiliations in this record was updated in December 2015. 25 The record was previously connected to the following departments: Nuclear Physics (Faculty of Technology) (011013007), 2002.

Hellén, H., Hakola, H., Haaparanta, S., Pietarila, H., and Kauhaniemi, M.: Influence of residential wood combustion on local air quality, Science of The Total Environment, 393, 283 – 290, https://doi.org/https://doi.org/10.1016/j.scitotenv.2008.01.019, http://www.sciencedirect.com/science/article/pii/S0048969708000454, 2008.

Holzinger, R., Warneke, C., Hansel, A., Jordan, A., Lindinger, W., Scharffe, D. H., Schade, G., and Crutzen, P. J.: Biomass burning as a source of formaldehyde, acetaldehyde, methanol, acetone, acetonitrile, and hydrogen cyanide, Geophysical Research Letters, 26, 1161– 1164, https://doi.org/10.1029/1999GL900156, https://agupubs.onlinelibrary.wiley.com/doi/abs/10.1029/1999GL900156, 1999.

Holzinger, R., Acton, W. J. F., Bloss, W. J., Breitenlechner, M., Crilley, L. R., Dusanter, S., Gonin, M., Gros, V., Keutsch, F. N., KiendlerScharr, A., Kramer, L. J., Krechmer, J. E., Languille, B., Locoge, N., Lopez-Hilfiker, F., Materic, D., Moreno, S., Nemitz, E., Quéléver,´ L. L. J., Sarda Esteve, R., Sauvage, S., Schallhart, S., Sommariva, R., Tillmann, R., Wedel, S., Worton, D. R., Xu, K., and Zaytsev, A.: Validity and limitations of simple reaction kinetics to calculate concentrations of organic compounds from ion counts in PTR-MS, Atmospheric Measurement Techniques Discussions, 2019, 1–29, https://doi.org/10.5194/amt-2018-446, https://www.atmos-meas-tech-discuss. net/amt-2018-446/, 2019.

Iinuma, Y., Engling, G., Puxbaum, H., and Herrmann, H.: A highly resolved anion-exchange chromatographic method for determination of saccharidic tracers for biomass combustion and primary bio-particles in atmospheric aerosol, Atmospheric Environment, 43, 1367 – 1371, https://doi.org/https://doi.org/10.1016/j.atmosenv.2008.11.020, http://www.sciencedirect.com/science/article/pii/ S1352231008010893, 2009.

Ito, K., Xue, N., and Thurston, G.: Spatial variation of PM2.5 chemical species and source-apportioned mass concentrations in New York City, Atmospheric Environment, 38, 5269 – 5282, https://doi.org/https://doi.org/10.1016/j.atmosenv.2004.02.063, http://www.sciencedirect.com/science/article/pii/S1352231004005655, particulate Matter: Atmospheric Sciences, Exposure and the Fourth Colloquium on PM and Human Health - Papers from the AAAR PM Meeting, 2004.

Kalogridis, A.-C., Vratolis, S., Liakakou, E., Gerasopoulos, E., Mihalopoulos, N., and Eleftheriadis, K.: Assessment of wood burning *versus* fossil fuel contribution to wintertime black carbon and carbon monoxide concentrations in Athens, Greece, Atmospheric Chemistry and Physics, 18, 10219–10236, https://doi.org/10.5194/acp-18-10219-2018, https://www.atmos-chem-phys.net/18/10219/2018/, 2018.

Khalil, M. and Rasmussen, R.: Tracers of wood smoke, Atmospheric Environment, 37, 1211 – 1222, https://doi.org/10.1016/S1352-2310(02)01014-2, http://www.sciencedirect.com/science/article/pii/S1352231002010142, james P. Lodge, Jr. Memorial Issue. Measurement Issues in Atmospheric Chemistry, 2003.

Kim, S., Karl, T., Helmig, D., Daly, R., Rasmussen, R., and Guenther, A.: Measurement of atmospheric sesquiterpenes by proton transfer reaction-mass spectrometry (PTR-MS), Atmospheric Measurement Techniques, 2, 99–112, https://doi.org/10.5194/amt-2-99-2009, https: //www.atmos-meas-tech.net/2/99/2009/, 2009.

Kotthaus, S, M-A Drouin, M Haeffelin, M Hervo, J Poltera, A Haefele and CSB Grimmond: Taking advantage of common automatic lidar and ceilometer (ALC) systems: tailored algorithms for the detection of the atmospheric boundary layer structure, in preparation.

Kotthaus, S, and CSB Grimmond: Atmospheric Boundary Layer Characteristics from Ceilometer measurements Part 1: A new method to track mixed layer height and classify clouds. Q. J. R. Meteorol. Soc., 144, 1525–1538, doi:10.1002/qj.3299, 2018.

Kotthaus, S, E O'Connor, Ch Münkel, C Charlton-Perez, M Haeffelin, AM Gabey, CSB Grimmond: Recommendations for processing atmospheric attenuated backscatter profiles from Vaisala CL31 ceilometers. Atmos. Meas. Tech., 9, 3769–3791, doi:10.5194/amt-9-3769-2016, 2016.

Lanz, V. A., Hueglin, C., Buchmann, B., Hill, M., Locher, R., Staehelin, J., and Reimann, S.: Receptor modeling of C2-C7 hydrocarbon sources at an urban background site in Zurich, Switzerland: changes between 1993-1994 and 2005-2006,

Atmospheric Chemistry and Physics, 8, 2313–2332, https://doi.org/10.5194/acp-8-2313-2008, https://www.atmos-chem-phys.net/8/2313/2008/, 2008.

Lindinger, W., Hansel, A., and Jordan, A.: On-line monitoring of volatile organic compounds at pptv levels by means of proton-transferreaction mass spectrometry (PTR-MS) medical applications, food control and environmental research, International Journal of Mass Spectrometry and Ion Processes, 173, 191 – 241, https://doi.org/https://doi.org/10.1016/S0168-1176(97)00281-4, http://www.sciencedirect.com/science/article/pii/S0168117697002814, 1998.

Maenhaut, W.: Source apportionment revisited for long-term measurements of fine aerosol trace elements at two locations in southern Norway, Nuclear Instruments and Methods in Physics Research Section B: Beam Interactions with Materials and Atoms, 417, 133 – 138, https://doi.org/https://doi.org/10.1016/j.nimb.2017.07.006, http://www.sciencedirect.com/science/article/pii/S0168583X17307097, pARTICLE INDUCED X-RAY EMISSION 15th International Conference on Particle Induced X-ray Emission, 2018.

Nalin, F., Golly, B., Besombes, J.-L., Pelletier, C., Aujay-Plouzeau, R., Verlhac, S., Dermigny, A., Fievet, A., Karoski, N., Dubois, P., Collet, S., Favez, O., and Albinet, A.: Fast oxidation processes from emission to ambient air introduction of aerosol emitted by residential log wood stoves, 143, 2016.

Nádudvari, d., Fabianska, M. J., Marynowski, L., Kozielska, B., Konieczy´ nski, J., Smołka-Danielowska, D., and´ Cmiel, S.: Distribution of´ coal and coal combustion related organic pollutants in the environment of the Upper Silesian Industrial Region, Science of The Total Environment, 628-629, 1462 – 1488, https://doi.org/https://doi.org/10.1016/j.scitotenv.2018.02.092, http://www.sciencedirect.com/science/article/pii/S0048969718304820, 2018.

Paatero, P. and Tapper, U.: Positive Matrix Factorization: A Non-Negative Factor Model with Optimal Utilization of Error Estimates of Data Values, in: Environmetrics, pp. 111–126, https://doi.org/10.1002/env.3170050203, 1994.

Panopoulou, A., Liakakou, E., Gros, V., Sauvage, S., Locoge, N., Bonsang, B., Psiloglou, B. E., Gerasopoulos, E., and Mihalopoulos, N.: Non-methane hydrocarbon variability in Athens during wintertime: the role of traffic and heating, Atmospheric Chemistry and Physics, 18, 16139–16154, https://doi.org/10.5194/acp-18-16139-2018, https://www.atmos-chem-phys.net/18/16139/2018/, 2018.

Petit, J.-E., Favez, O., Sciare, J., Canonaco, F., Croteau, P., Mocnik, G., Jayne, J., Worsnop, D., and Leoz-Garziandia, E.: Submicron˘ aerosol source apportionment of wintertime pollution in Paris, France by double positive matrix factorization (PMF2) using an aerosol chemical speciation monitor (ACSM) and a multi-wavelength Aethalometer, Atmospheric Chemistry and Physics, 14, 13773–13787, https://doi.org/10.5194/acp-14-13773-2014, https://www.atmos-chem-phys.net/14/13773/2014/, 2014.

Petit, J.-E., Favez, O., Sciare, J., Crenn, V., Sarda-Estève, R., Bonnaire, N., Mocnik, G., Dupont, J.-C., Haeffelin, M., and Leoz-Garziandia, E.: Two years of near real-time chemical composition of submicron aerosols in the region of Paris using an Aerosol Chemical Speciation Monitor (ACSM) and a multi-wavelength Aethalometer, Atmospheric Chemistry and Physics, 15, 2985–3005, https://doi.org/10.5194/acp15-2985-2015, https://www.atmos-chem-phys.net/15/2985/2015/, 2015.

Petit, J.-E., Amodeo, T., Meleux, F., Bessagnet, B., Menut, L., Grenier, D., Pellan, Y., Ockler, A., Rocq, B., Gros, V., Sciare, J., and Favez, O.: Characterising an intense PM pollution episode in March 2015 in France from multi-site approach and near real time data: Climatology, variabilities, geographical origins and model evaluation, Atmospheric Environment, 155, 68 – 84, https://doi.org/https://doi.org/10.1016/j.atmosenv.2017.02.012, http://www.sciencedirect.com/science/article/pii/ S1352231017300821, 2017.

Puxbaum, H., Caseiro, A., Sánchez-Ochoa, A., Kasper-Giebl, A., Claeys, M., Gelencsér, A., Legrand, M., Preunkert, S., and Pio, C.. Levoglucosan levels at background sites in Europe for assessing the impact of biomass combustion on the European aerosol background. Journal of Geophysical Research: Atmospheres, 112(D23), 2007.

R Core Team. R : A Language and Environment for Statistical Computing. R Foundation for Statistical Computing, Vienna, Austria, 2018.

Rolph, G.: Real-time Environmental Applications and Display sYstem (READY), NOAA Air Resources Laboratory, 2016. Sandradewi, J., Prévôt, A. S. H., Szidat, S., Perron, N., Alfarra, M. R., Lanz, V. A., Weingartner, E., and Baltensperger, U.: Using Aerosol Light Absorption Measurements for the Quantitative Determination of Wood Burning and Traffic Emission Contributions to Particulate Matter, Environmental Science & Technology, 42, 3316–3323, https://doi.org/10.1021/es702253m, https://doi.org/10.1021/es702253m, pMID: 18522112, 2008.

Sauvage, S., Plaisance, H., Locoge, N., Wroblewski, A., Coddeville, P., and Galloo, J.: Long term measurement and source apportionment of non-methane hydrocarbons in three French rural areas, Atmospheric Environment, 43, 2430 – 2441, https://doi.org/https://doi.org/10.1016/j.atmosenv.2009.02.001, http://www.sciencedirect.com/science/article/pii/S1352231009001204, 2009.

Schauer, J. J., Kleeman, M. J., Cass, G. R., and Simoneit, B. R. T.: Measurement of Emissions from Air Pollution Sources. 3. C1-C29 Organic Compounds from Fireplace Combustion of Wood, Environmental Science and Technology, 35, 1716–1728, https://doi.org/10.1021/es001331e, http://dx.doi.org/10.1021/es001331e, pMID: 11355184, 2001.

Schwartz, J., Dockery, D. W., and Neas, L. M.: Is Daily Mortality Associated Specifically with Fine Particles?, Journal of the Air & Waste Management Association, 46, 927–939, https://doi.org/10.1080/10473289.1996.10467528, https://doi.org/10.1080/10473289. 1996.10467528, pMID: 28065142, 1996.

Sciare, J., D'Argouges, O., Sarda-Esteve, R., Gaimoz, C., Dolgorouky, C., Bonnaire, N., Favez, O., Bonsang, B., and Gros, V.: Large contribution of water-insoluble secondary organic aerosols in the region of Paris (France) during

wintertime, Journal of Geophysical Research: Atmospheres, 116, D22203, https://doi.org/10.1029/2011JD015756, https://hal-ineris.archives-ouvertes.fr/ineris-00963327, 2011.

Seco, R., Peñuelas, J., Filella, I., Llusia, J., Schallhart, S., Metzger, A., Müller, M., and Hansel, A.: Volatile organic compounds in the western Mediterranean basin: urban and rural winter measurements during the DAURE campaign, Atmospheric Chemistry and Physics, 13, 4291–4306, https://doi.org/10.5194/acp-13-4291-2013, https://www.atmos-chem-phys.net/13/4291/2013/, 2013.

Sällsten, G., Gustafson, P., Johansson, L., Johannesson, S., Molnár, P., Strandberg, B., Tullin, C., and Barregard, L.: Experimental Wood Smoke Exposure in Humans, Inhalation Toxicology, 18, 855–864, https://doi.org/10.1080/08958370600822391, https://doi.org/10.1080/ 08958370600822391, pMID: 16864403, 2006.

Stein, A., Draxler, R., Rolph, G., Stunder, B., Cohen, M., and Ngan, F.: NOAA's HYSPLIT atmospheric transport and dispersion modeling system, Bull. Amer. Meteor. So, 96, 2059–2077, 2015.

Taipale, R., Ruuskanen, T. M., Rinne, J., Kajos, M. K., Hakola, H., Pohja, T., and Kulmala, M.: Technical Note: Quantitative long-term measurements of VOC concentrations by PTR-MS measurement, calibration, and volume mixing ratio calculation methods, Atmospheric Chemistry and Physics, 8, 6681–6698, https://doi.org/10.5194/acp-8-6681-2008, https://www.atmos-chem-phys.net/8/6681/2008/, 2008.

Valach, A., Langford, B., Nemitz, E., MacKenzie, A., and Hewitt, C.: Concentrations of selected volatile organic compounds at kerbside and background sites in central London, Atmospheric Environment, 95, 456 – 467, https://doi.org/https://doi.org/10.1016/j.atmosenv.2014.06.052, http://www.sciencedirect.com/science/article/pii/S1352231014004981, 2014.

Waked, A., Sauvage, S., Borbon, A., Gauduin, J., Pallares, C., Vagnot, M., Leonardis, T., and Locoge, N.: Multi-year levels and trends of non-methane hydrocarbon concentrations observed in ambient air in France, Atmospheric Environment, 141, 263–275, 2016.

Zhang, Y., Favez, O., Canonaco, F., Liu, D., Mocnik, G., Amodeo, T., Sciare, J., Prevot, A., Gros, V., and Albinet, A.: Evidence of majorˇ secondary organic aerosol contribution to lensing effect black carbon absorption enhancement, npj Climate and Atmospheric Science, 1, https://doi.org/10.1038/s41612-018-0056-2, 2018.

Zhao, J. and Zhang, R.: Proton transfer reaction rate constants between hydronium ion (H_3O^+) and volatile organic compounds (VOCs), Atmospheric Environment, 38, 2177–2185, https://doi.org/10.1016/j.atmosenv.2004.01.019, 2004.

Appendix A: Map of the considered sites in the present work

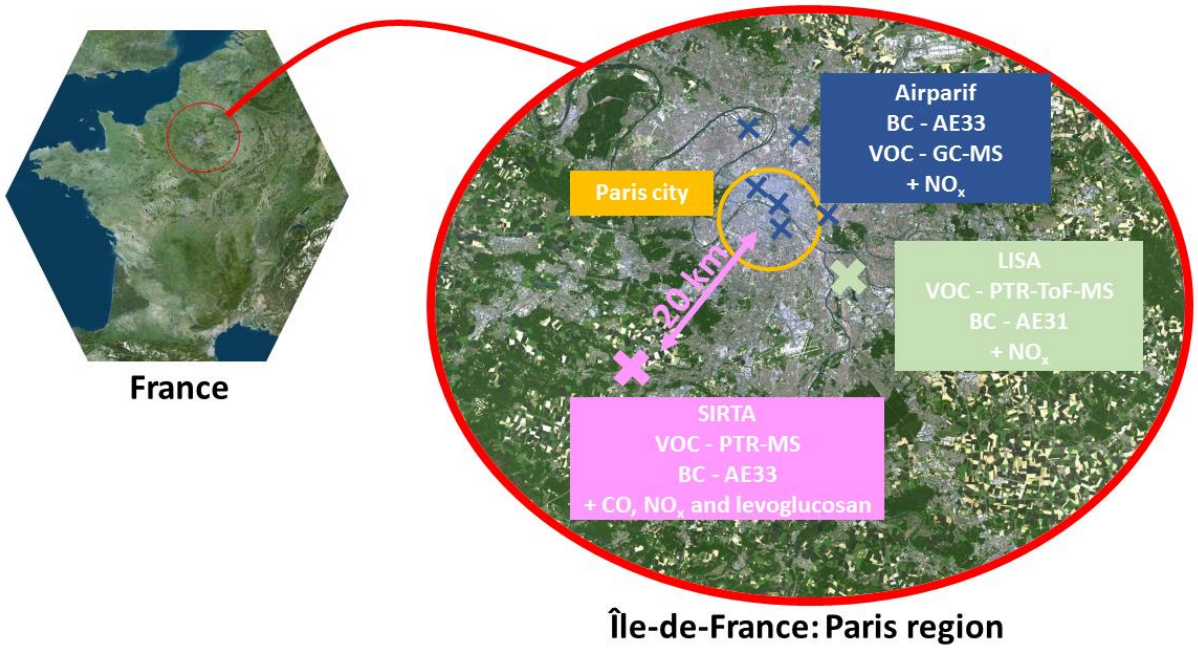

955 **Figure A1 Considered sites in the present work: SIRTA (30 Nov. 2017 – 12 March 2018 for VOCs, continuous for the other pollutants, pink cross), LISA (2 Feb. – 12 March 2018, white cross), AIRPARIF (continuous, blue crosses).**

Appendix B: PTR-MS calculation

B1 Normalization and blank subtraction

The raw data from PTR-MS are in counts per second (CPS) for which the value depends on ionisation processes. This is why it needs to be normalised by the primary ion CPS. The normalized counts per second (NCPS) are obtained using this formula:

$$X_{NCPS} = 10^6 \frac{X_{CPS}}{500 \times {H_3O^+}_{CPS} + (H_3O^+H_2O)_{CPS}}$$

The second step of the data processing is the blank subtraction. The blanks are scheduled every 13 h and last 1 h. The last measurement of the blank is removed (because the atmospheric measurements resume), and the first measurements of a blank period are not taken into account in order not to be impacted by memory effect. In this way, only the 35 last minutes of the blank are considered. The blanks are interpolated using the smooth.spline function from R language and the parameter "spar" set to 0.5.

B2 Calibration

The calibrations were conducted using a National Physical Laboratory (NPL) gas mixture. The canister is diluted from the initial concentration of 1 ppm to the desired concentration for the five calibration steps (1 ppb, 2 ppb, 4 ppb, 8 ppb and16 ppb). Each step lasts one hour. Eleven protonated masses were calibrated: 33-methanol, 42-acetonitrile, 45-acetaldehyde, 15 57-propenal, 59-acetone, 69-isoprene, 71-crotonaldehyde, 73-butanone, 79-benzene, 93-toluene and 107-xylenes.

B3 Transmission curve

The other masses were quantified with the transmission curve. For each calibrated mass, the transmission was defined according to Taipale et al. (2008) as:

$$Tr_{m/z} = 10^9 \frac{P_{drift}}{10^6 \, P_0 \, k L_{drift} N^2} \times S_{m/z}$$

Where P_{drift} is the pressure into to drift tube, P0 the normalized pressure, µ0 is the ion mobility of the primary ions, N_0 is the number density of air, E is the electric field in the drift tube, k is the proton transfer reaction rate coefficient, L_{drift} is the drift tube length, N is the number density in the drift tube, and Sm/z is the sensibility or the calibration coefficient for each mass. Once the transmission values are known for the calibrated masses, an interpolation leads to approximate the values for any mass. Then, an approximation of the concentration values is deduced from the following formula:

$$C_{m/z} = \frac{NCPS_{m/z}}{Tr_{m/z}} \times \frac{10^9 P_{drift}}{10^6 P_0} \times \frac{\mu_0 N_0 E}{k L_{drift} N^2}$$

Where $NCPS_{m/z}$ is the signal for the mass m/z in NCPS and $Tr_{m/z}$ the interpolated transmission for the mass m/z.

B4 Uncertainties calculation

The uncertainties are calculated according to the ACTRIS guidelines as:

$$Uncertainty^2 = Precision^2 + SystError^2 \quad (A4)$$

Where the precision and the systematic error are calculated as:

$$Precision = \frac{1}{3} \times LOD + C \times CV_{target}$$

$$SystError^2 = StandardPrecision^2 + StandardDilutionPrecision^2$$

Where LOD is the limit of detection set as 3 times the standard deviation of the blank and CV_{target} is the coefficient of variation of the target gas. The precision on the standard and the standard dilution precision are 5 %.

Appendix C: BC corrections

C1 Measurement principle and compensation

The BC measurement principle is based on an optical absorption quantification. The light attenuation due to the particles is calculated as follows:

$$ATN = 100 \times \ln\left(\frac{I_0}{I}\right)$$

Where I_0 is the reference light intensity and I the light intensity of the stream that crossed the collecting tape loaded with aerosols.

Corrections due to experimental artefacts (air flow fluctuation, multiple scattering parameter, shadowing effect) were applied to ATN in order to obtain the "true" absorption coefficients b_{abs}.

C2 Validation

A validation process, based on the one used by LCSQA (central laboratory for air quality monitoring[8]) was applied to the data, as it was done in Petit et al. (2017). Three steps were considered. First, all the negative values were invalidated. Then, the spectral dependency was checked looking at the linear relation between $\ln(b_{abs})$ and the seven wavelengths. Each measurement was validated if the slope (the Angstrom exponent, $-\alpha$) was between - 0.75 and - 3; and the coefficient of determination (r^2) above or equal to 0.9.

At the end, 88 % of the data were validated for the 1 min time step.

C3 Source apportionment model

The model proposed by Sandradewi et al. (2008), allowing apportioning for the wood burning and traffic parts, is based on the three following equations:

$$b_{abs}(\lambda) = b_{abs,traffic}(\lambda) + b_{abs,wb}(\lambda)$$

[8] www.lcsqa.org

$$\frac{b_{abs,traffic}(\lambda_{UV})}{b_{abs,traffic}(\lambda_{IR})} = \frac{(\lambda_{UV})^{-\alpha_{traffic}}}{(\lambda_{IR})}$$

$$\frac{b_{abs,wb}(\lambda_{UV})}{b_{abs,wb}(\lambda_{IR})} = \frac{(\lambda_{UV})^{-\alpha_{wb}}}{(\lambda_{IR})}$$

Where λ_{UV} and λ_{IR} are ultraviolet and infrared wavelengths (respectively 470 and 950 nm), and $\alpha_{traffic}$ and α_{wb} are the Angstrom exponent for the fossil fuel and wood burning fractions.

A combination of these three equations leads to the following formula:

$$b_{abs,wb}(\lambda_{UV}) = \frac{b_{abs}(\lambda_{UV}) - \frac{\lambda_{UV}}{\lambda_{IR}}^{-\alpha_{traffic}}}{1 - \frac{\lambda_{UV}}{\lambda_{IR}}^{-\alpha_{traffic}} \frac{\lambda_{UV}}{\lambda_{IR}}^{-\alpha_{wb}}}$$

The most important step was to determine the Angstrom exponents $\alpha_{traffic}$ and α_{wb}, initially set to 1 and 2 into the instrument software. The Angstrom exponent distribution displayed in Figure B1, shows that the percentile 98 % are 1.07 and 1.96. These values were retained as respectively $\alpha_{traffic}$ and α_{wb}. These values are slightly higher the one found in Zhang et al. (2018), which may be related to the fact that this dataset is much shorter in time and focusing on a single season only.

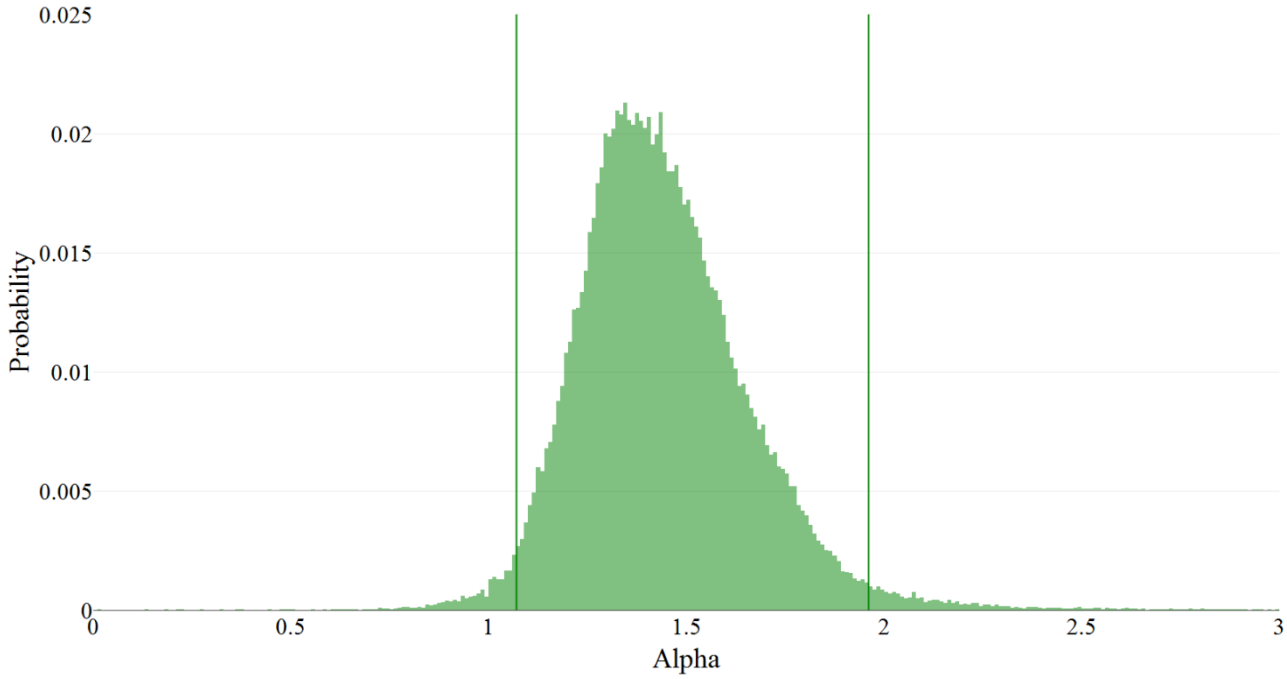

Figure C1 Angstrom exponent repartition and percentile 98.

1045

The same methodology (validation, source apportionment, choice for alpha, etc.) was applied for the Airparif and LISA stations.

Appendix D: PMF settings

D1 VOC settings: bad, weak or strong

The Environmental Protection Agency (EPA) PMF V5.0 model allows classifying the variables as "strong", "weak" or "bad" depending on the reliability of the measurements. Basically, a strong variable is used with given uncertainties, the uncertainties are tripled for a weak variable, and a bad variable is removed from the dataset.

Quite a lot of compounds were considered in the PMF model, but not all of them were as reliable as one another. For instance, the calibrated masses were more certain than the non-calibrated masses. And among the calibrated masses, the measurement is more robust for some of them. The VOCs classified as "strong" were methanol, acetaldehyde, acetone, benzene and toluene.

This choice was made because these masses had the lowest uncertainties among the calibrated masses (except for acrolein, which suffered from outliers during the campaigns and was then tagged as "weak"). All the other VOCs were classified as "weak".

The residuals analysis showed that all the VOCs classified as strong had well distributed residuals (Figure C1).

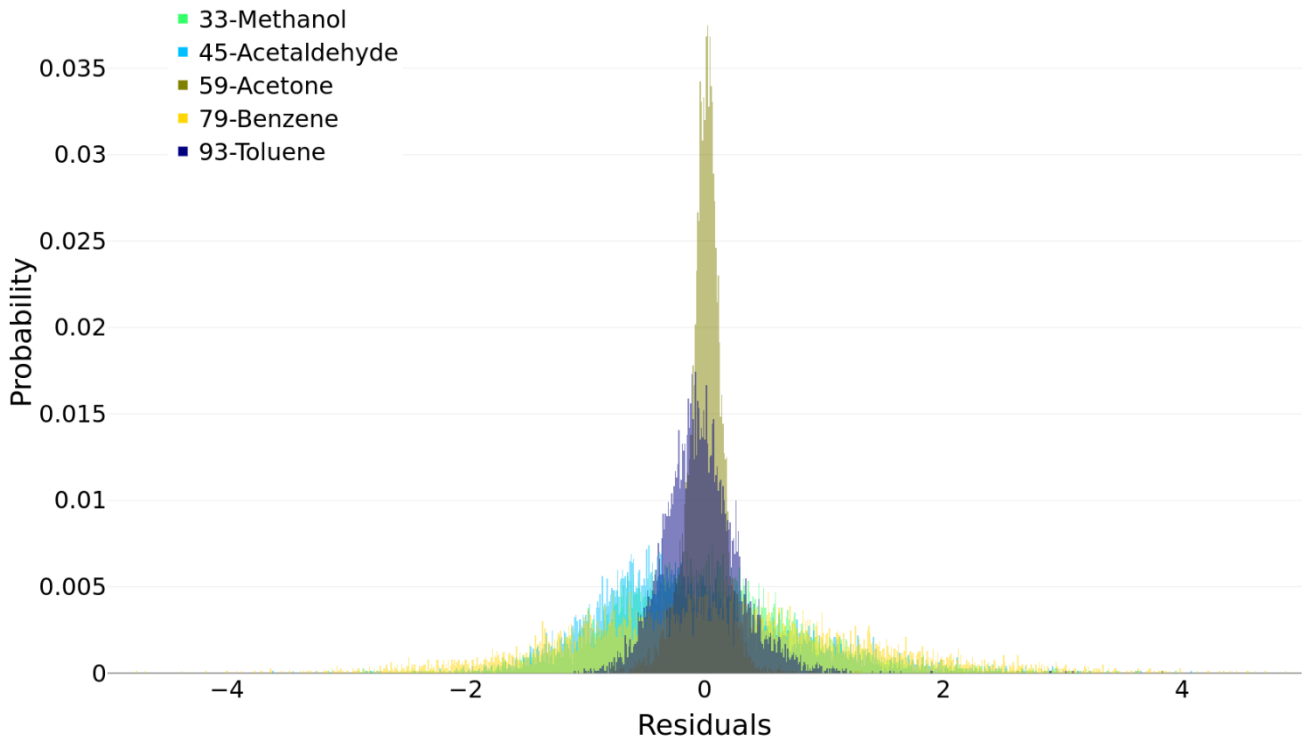

Figure D1 Scaled residuals repartition for the VOCs classified "strong".

D2 Determination of the number of factors

Determining the most relevant number of factors is a key point in the use of the PMF model. Different approaches are possible to reach to most appropriate factor number. In this study, it was chosen to primary consider the physical meaningfulness of the results as it was done in some studies (Lanz et al., 2008). Several computations were conducted in order to make the best choice concerning the number of factors.

The 3-factor solution obtained with a 20-run simulation was retained. The 4-factor solution led to a benzene rich factor without atmospheric meaning. Adding a fifth factor has the effect of splitting the wood burning factor in two, which does not make sense. Solutions including more factors led to non-physically interpretable solutions.

Appendix E: Overview of results at SIRTA

	Species	m/z	25th	Median	Mean	sd	75th	Bckgr.
Carbonyl	Formaldehyde	31	0.281	0.132	0.373	0.368	0.531	0.163
	Acetaldehyde	45	0.626	0.374	0.822	0.635	1.111	0.332
	Propenal	57	1.276	0.975	1.453	0.777	1.723	1.094
	Acetone	59	1.256	0.898	1.481	0.901	1.836	0.865
	Butenal	71	0.116	0.034	0.155	0.151	0.209	0.093
	MEK	73	0.480	0.196	0.538	0.365	0.719	0.262
	Hexenal + monoterp.	81	0.159	0.085	0.191	0.175	0.252	0.140
	Methylbutenone	85	0.192	0.102	0.247	0.211	0.335	0.146
	Butandione	87	0.307	0.175	0.358	0.262	0.483	0.250
Alcohol	Methanol	33	1.317	0.842	1.573	1.084	2.058	0.728
Nitrile	Acetonitrile	42	0.107	0.076	0.119	0.081	0.144	0.099
Acid	Acetic acid	61	0.786	0.439	1.062	0.965	1.377	0.362
Furans	Furan	69	0.285	0.083	0.375	0.339	0.505	0.198
	Methylfuran	83	0.220	0.122	0.277	0.243	0.365	0.188
	Furfural	97	0.395	0.119	0.522	0.502	0.685	0.196
	Furandione	99	0.231	0.097	0.283	0.222	0.402	0.184
Aromatic	Benzene	79	0.633	0.379	0.751	0.491	1.033	0.363

	Toluene	93	0.597	0.299	0.808	0.747	1.103	0.352
	C8-arom.	107	0.575	0.576	0.861	0.649	0.575	0.594
	C9-arom.	121	0.765	0.334	0.916	0.720	1.268	0.552
O-arom.	Phenol	95	0.134	0.054	0.170	0.144	0.234	0.126
	Benzenediol	111	0.137	0.137	0.322	0.257	0.440	0.221
Others	Propene+	43	0.843	0.546	1.027	0.715	1.312	0.454
	Chlorobenzene	113	0.240	0.066	0.287	0.235	0.405	0.215
	Methylacetate	75	0.239	0.133	0.309	0.264	0.408	0.147
Total VOC			5.666	9.57	10.917	8.992	15.481	7.388
	BC_{wb}	-	59	115	177	181	237	67
	$BC_{traffic}$	-	100	230	392	430	541	124
	BC_{tot}	-	168	364	562	544	812	182

Table E1: Main descriptive statistics for BC (ng.m^{-3}) and VOC (µg.m^{-3}) measurements during the campaign. m/z is the protonated mass, 25th is the 25th percentile, sd is the standard deviation and 75th is the 75th percentile, Bckgr. is for the background period from 15 to 25 January 2018, the mean values are considered.

Appendix F: Comparison between results from this study and from other European works

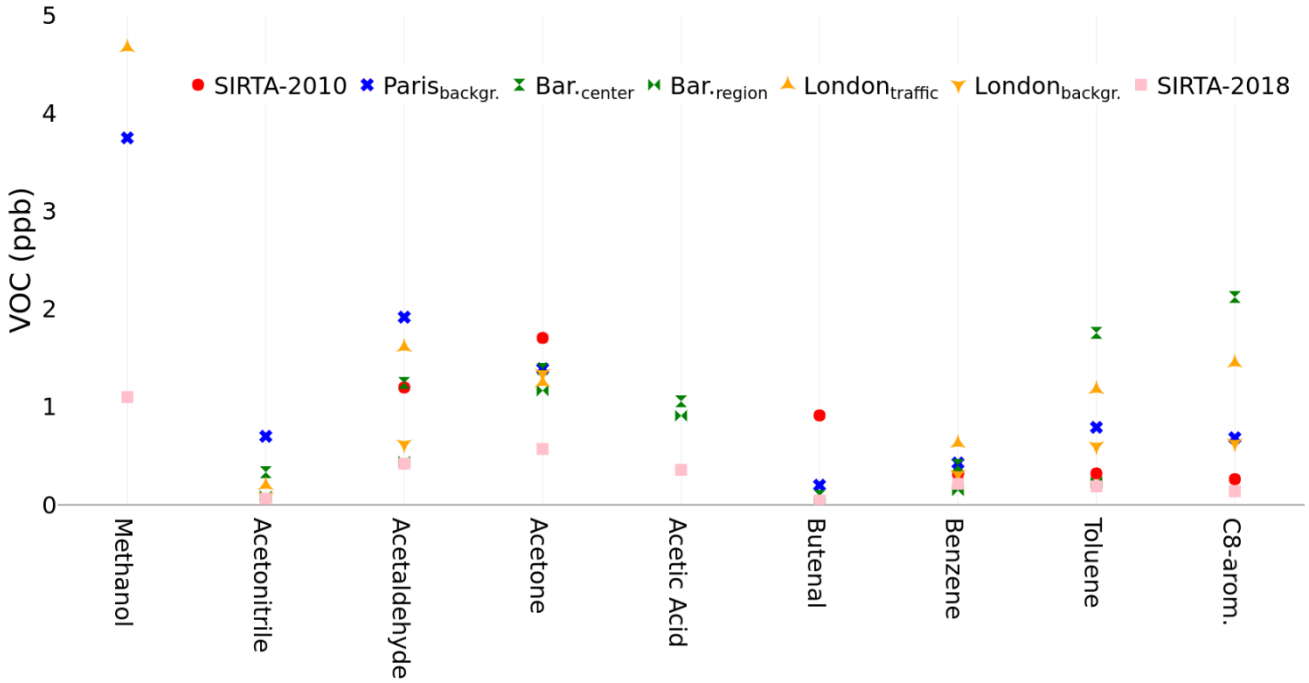

Figure F1 Comparison of mean concentrations of a selection of VOCs between the present study (SIRTA-2018) and literature. "backgr." stands for "background" and "Bar." for "Barcelona". SIRTA-2010: Ait-Helal et al., 2014, Paris$_{backgr.}$: Baudic et al., 2016, Bar.$_{center}$ and Bar.$_{region}$: Seco et al., 2013, London$_{traffic}$ and London$_{backgr.}$: Valach et al., 2014. The whole period is considered for the present study. For the other studies, the considered periods are: Ait-Helal et al. (2014) 15 January - 15 February 2010, Baudic et al. (2016) January - March 2010, Seco et al. (2013) 26 February 2009 - 26 March 2009, Valach et al. (2014) 16 January – 7 February 2012.

VOC (mean ppb)	This study	Ait-Helal et al. (2014)	Baudic et al. (2016)
	SIRTA	SIRTA	Paris city centre
	Winter 2018	Winter 2010[1]	Winter 2010[2]
33-Methanol	1.102	-	3.748
42-Acetonitrile	0.065	-	0.701
45-Acetaldehyde	0.420	1.199	1.917

59-Acetone	0.572	1.705	1.391		
61-Acetic acid	0.358	-	-		
71-Butenal	0.044	0.914[a]	0.202		
79-Benzene	0.215	0.316	0.428		
93-Toluene	0.190	0.321	0.792		
107-C8-arom.	0.139	0.263[b]	0.685		

VOC (mean ppb)	This study	Seco et al. (2013)[c]	Seco et al. (2013)[c]	Valach et al. (2014)	
	SIRTA	Barcelona centre	Montseny (rural)	London traffic	
	Winter	Winter 2009[3]	Winter 2009[3]	Winter 2012[4]	
33-Methanol	1.102	-	1.279 - 2.704	4.67	
42-Acetonitrile	0.065	0.209 - 0.460	0.075 - 0.101	0.20	
45-Acetaldehyde	0.420	0.804 - 1.688	0.227 - 0.657	1.61	
59-Acetone	0.572	1.131 - 1.645	0.787 - 1.547	1.25	
61-Acetic acid	0.358	0.728 - 1.389	0.393 - 1.428	-	
71-Butenal	0.044	0.068 - 0.115	0.011 - 0.047	-	-
79-Benzene	0.215	0.225 - 0.588	0.105 - 0.190	0.63	0.31
93-Toluene	0.190	0.805 - 2.711	0.057 - 0.408	1.18	0.60
107-C8-arom.	0.139	0.861 - 3.386	0.031 - 0.249	1.45	0.63

Table F1: Comparison of mean concentrations of a selection of VOCs between the present study and literature. The whole period is considered for the present study. For the other studies, the considered period is specified. More precisely the dates are: [1]15 January - 15 February 2010, [2]January - March 2010, [3]26 February 2009 - 26 March 2009, [4]16 January – 7 February 2012. [a]: sum of MVK and butenal. [b]: sum of ethylbenzene, m-p-xylene and o-xylene. [c]: hourly averages minimum - hourly averages maximum.

Ait-Helal et al. (2014) conducted a study at SIRTA, in 2010 while the investigations by Baudic et al. (2016) took place in Paris city centre in 2010. Two other studies used for comparison (Seco et al., 2013; Valach et al., 2014) were conducted in European cities similar to Paris (Barcelona, Spain, and London, UK, respectively), both including a comparison between two contrasting locations. Seco et al. (2013) analysed measurements taken at a central urban location in Barcelona and a rural site (Montseny) in winter 2009, while Valach et al. (2014) compared a traffic and a background site in London during winter 2012. For comparison purpose, the winter period matching the period of our study was considered.

Measurements from our study were below the levels at the London background site for all VOCs. SIRTA showed levels very close to the observations at Montseny (rural area). Only the mean benzene concentration was slightly higher (0.215 ppb *versus* 0.105 - 0.190 ppb) at SIRTA.

Appendix G: BC and VOCs time series for the entire campaign at SIRTA.

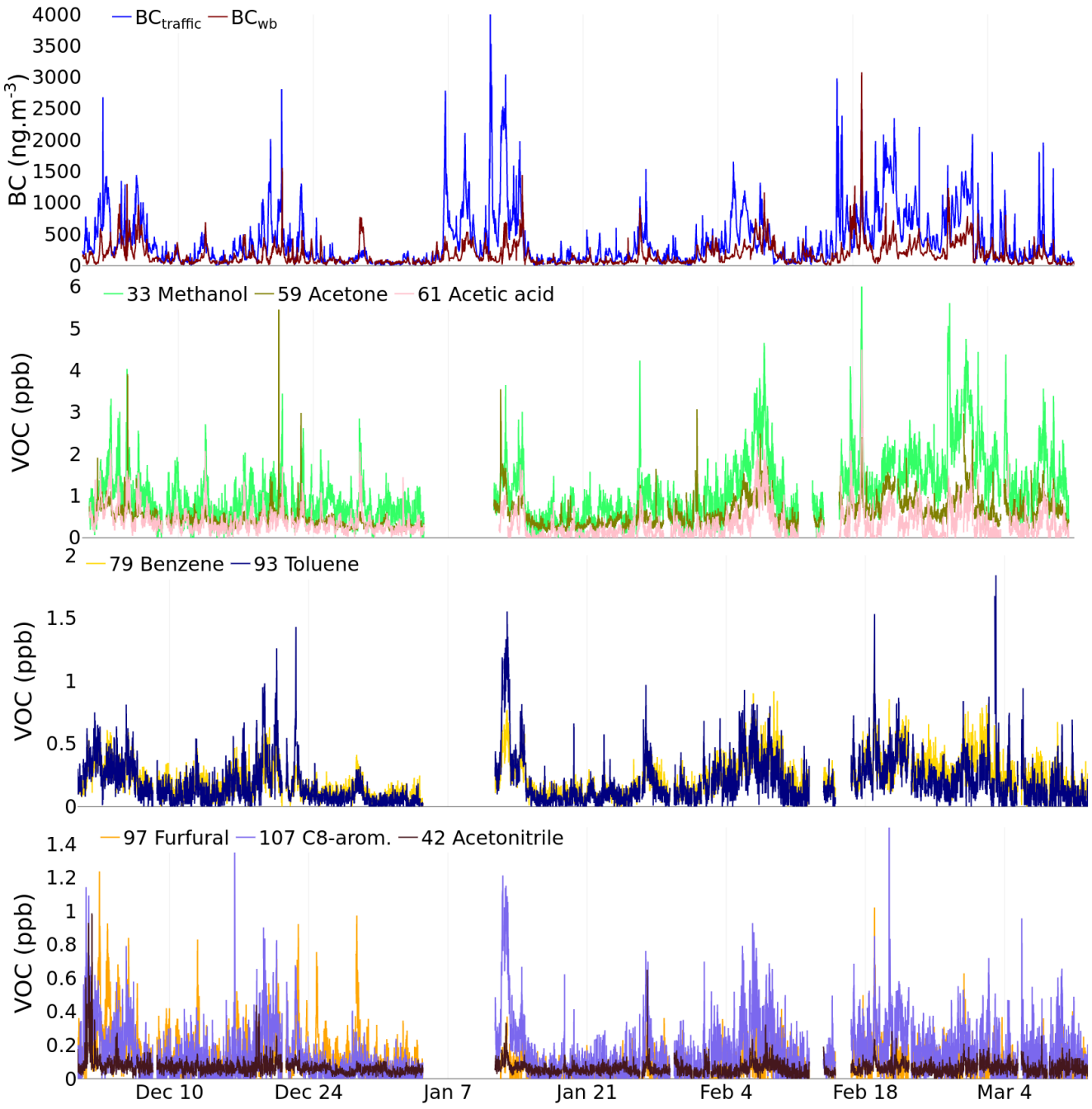

Figure G1 BC_{wb}, $BC_{traffic}$ and VOCs (selection of masses) time series for the whole campaign (30 November 2017 – 12 March 2018).

Appendix H: Air mass back-trajectories

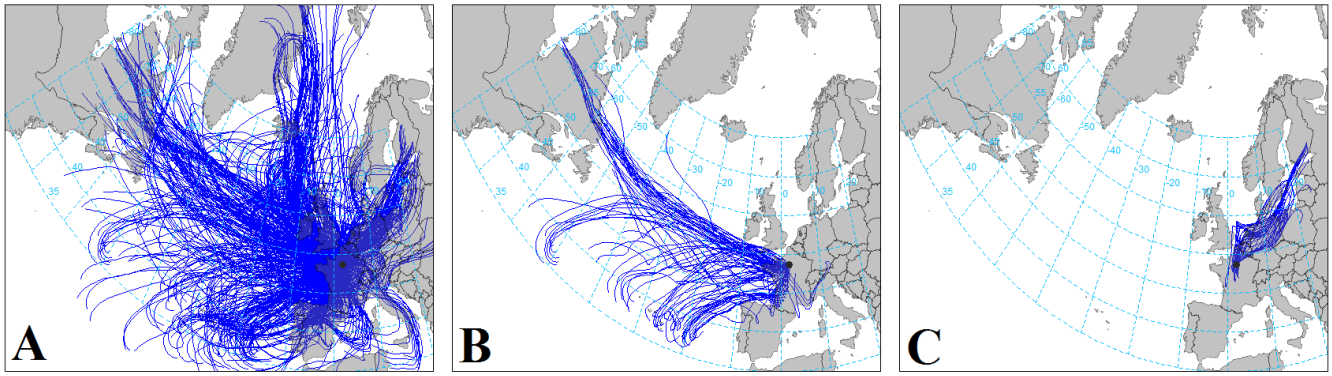

Figure H1 Air mass back-trajectories. Panel A: the whole campaign (30 Nov. 2017 - 12 March 2018), panel B: the background period (15 Jan. - 25 Jan. 2018), and panel C: the polluted episode (5 Feb. - 9 Feb. 2018).

A typical background (low polluted) period occurred from 15 to 25 January. During this interval, more than 99 % of the time, the sum of all VOCs was below the average sum for the whole campaign (7.39 µg.m^{-3} *vs* 10.91 µg.m^{-3}). For BC, more than 98 % of the time, BC_{tot} was below the mean value (182 ng.m^{-3} *vs* 562 ng.m^{-3}). On the contrary, the period spanning from 5 to 9 February was characterized by high pollution levels. More than 92 % of the time, the sum of the measured VOCs was above the overall mean and 87 % of the time BC_{tot} exceeded the campaign average.

These contrasting periods are mainly driven by their respective air masses origins (Figure H1). Over the whole campaign period, air masses advected to the Paris region from any wind direction have been observed, with a prevalence for westerly flow (panel A). For the background period, the majority of the air masses came from the Atlantic region (panel B), whereas the polluted episode was characterized by continental air masses (panel C). This observation is consistent with previous studies (e.g., Gros et al., 2011; Petit et al., 2014) which already highlighted the importance of air mass origin for pollutant levels.

Other meteorological parameters also played a key role in the ambient pollutant levels. The average wind speed for the whole campaign was 3.3 m.s^{-1}, 5.2 m.s^{-1} during the background period, and 1.7 m.s^{-1} during the polluted episode. The mixed layer height (MLH) was another important contributor to the pollution episode as the average maximum daytime MLH was lower (680 m) compared to the overall campaign (950 m). During the background period, mean maximum daytime MLH (900 m) was similar to the general winter conditions; however, during these January days, frequent rainfall likely causes uncertainty in the MLH results. The precipitation parameter further indicates that wet deposition likely played an important role. The temperature was significantly higher during the background period (mean 8 °C) than during the polluted phase (mean 1 °C).

These contrasts in air mass origin and meteorological parameters highlight that weather conditions are important drivers for ambient concentrations, in addition to the emissions' variability impact on concentration dynamics. Strong winds and vertical dilution within the mixed layer enhance pollutant dispersion. Furthermore, low temperatures are favourable conditions for pollutant accumulation while enhancing wood burning activities.

Appendix I: Cumulated traffic jams length and $BC_{traffic}$ (two-weeks sample).

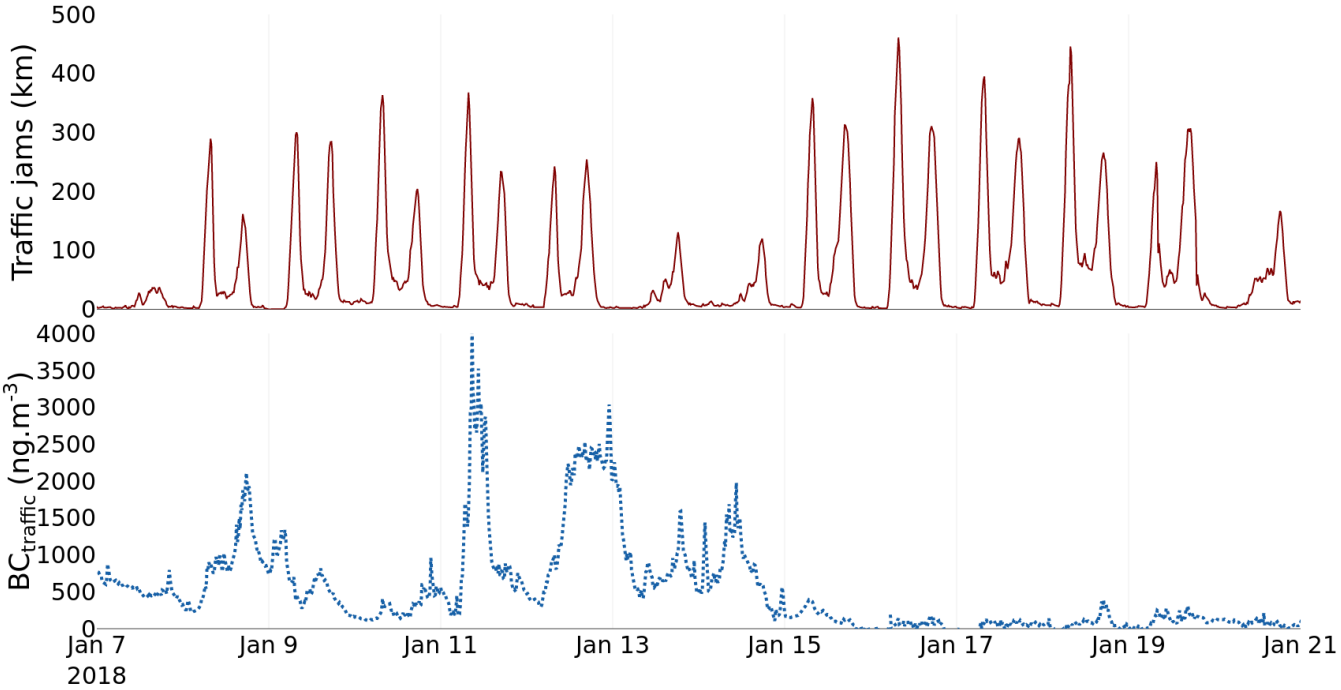

1155

Figure I1 Cumulated traffic jams length and $BC_{traffic}$ (two-week sample).

Appendix J: Diurnal cycles

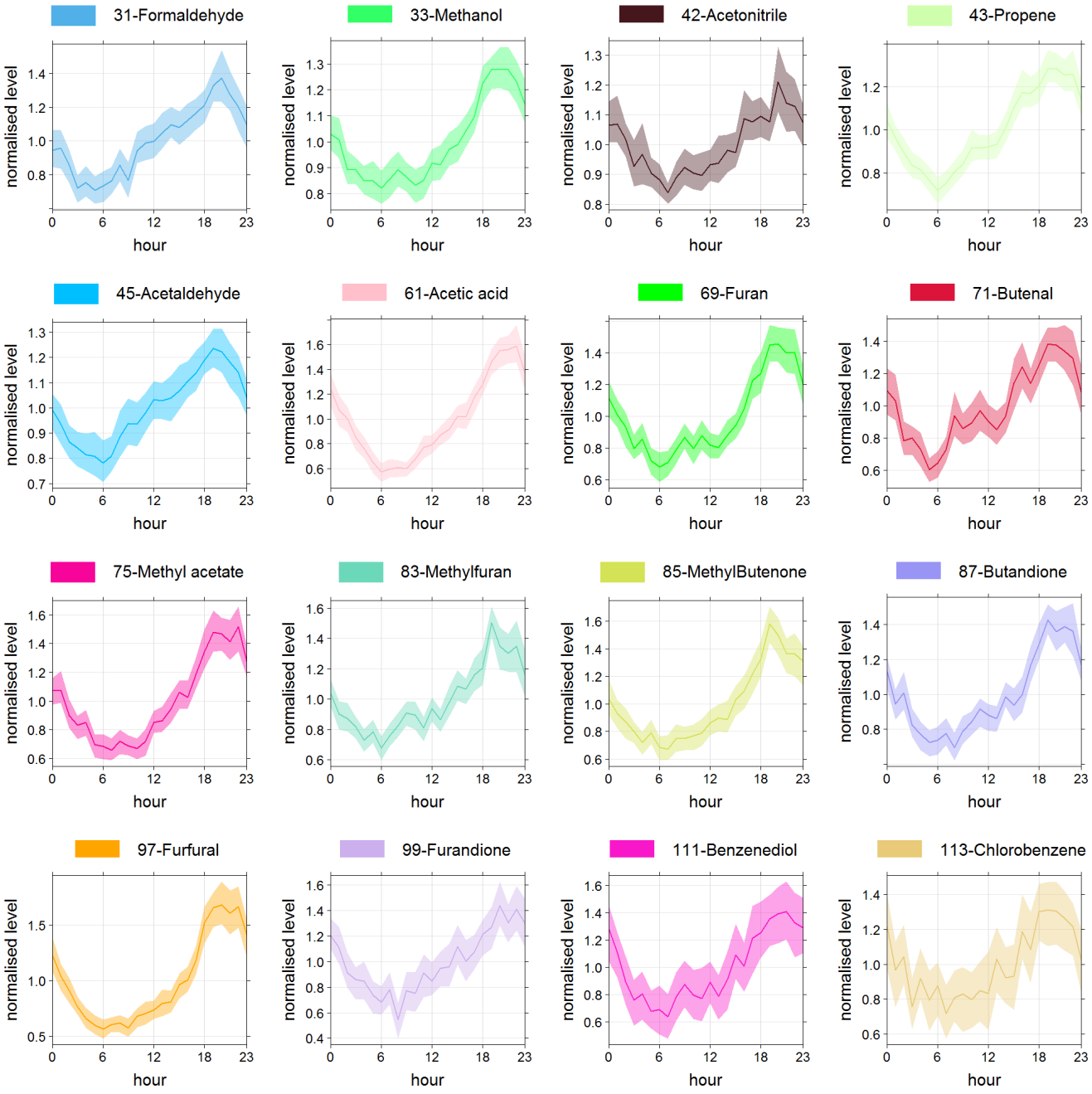

Figure J1 Diurnal cycles of the VOCs characterized by a wood burning pattern (plotted individually).

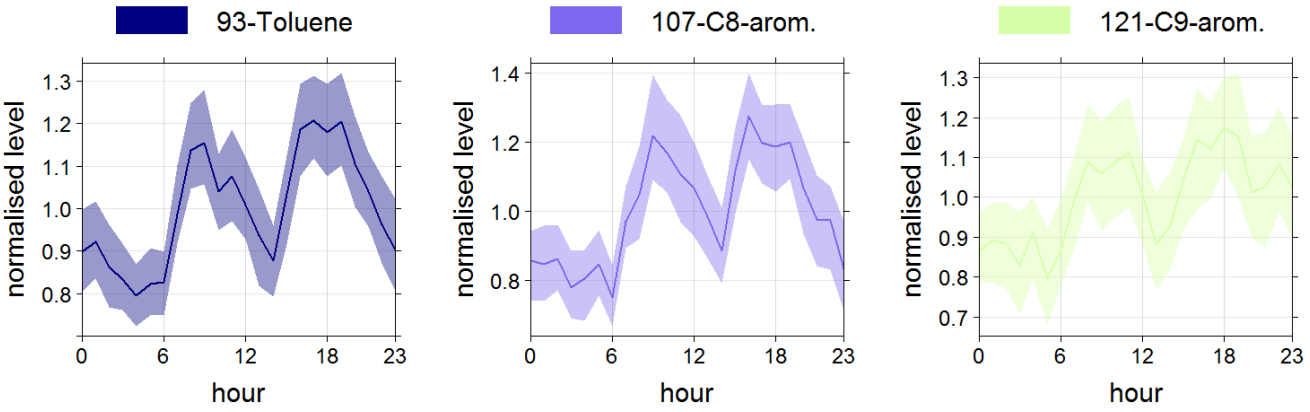

Figure J2 Diurnal cycles of the VOCs characterized by a traffic pattern (plotted individually).

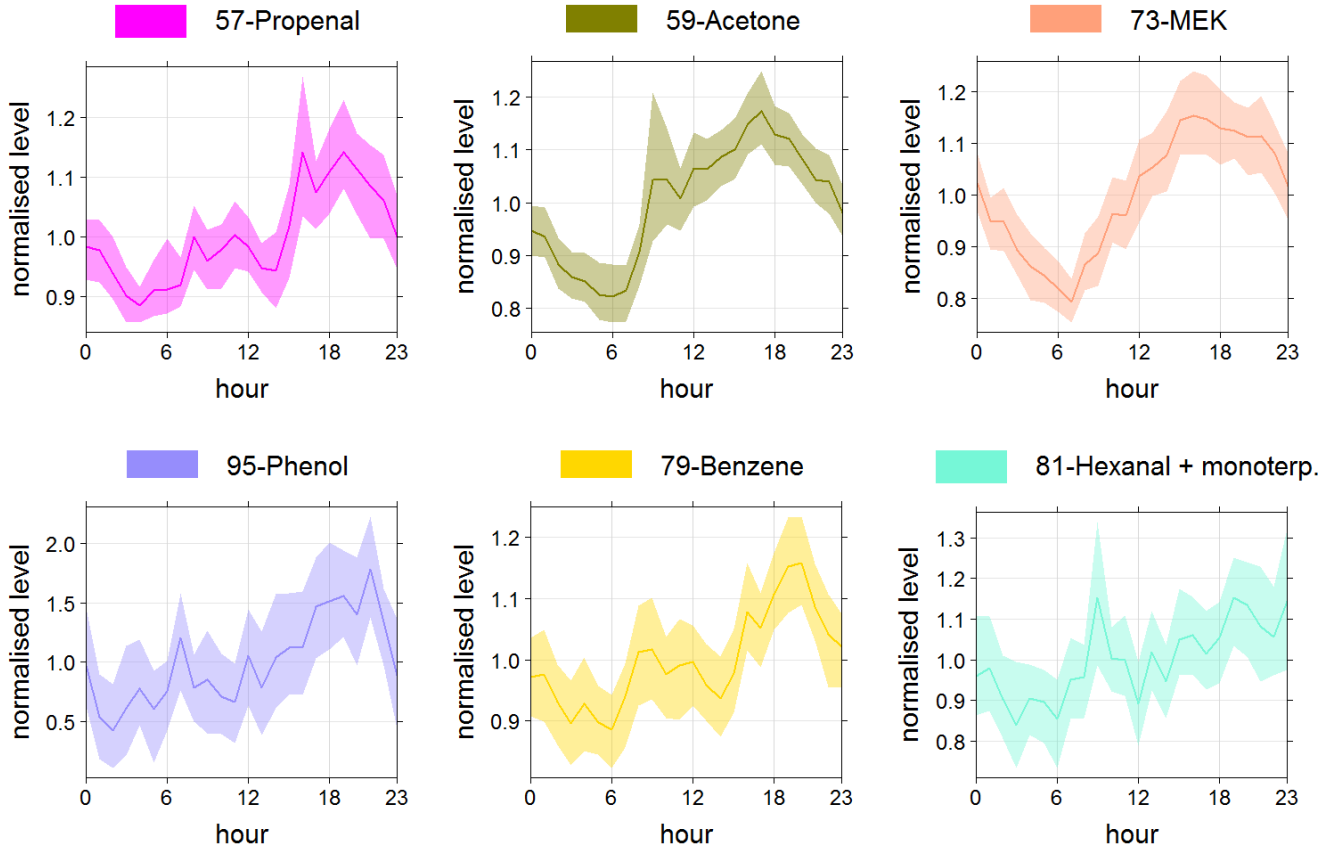

Figure J3 Diurnal cycles of the VOCs not classified with the diurnal cycle study (plotted individually).

Appendix K: BC and NO_x distribution for all the stations

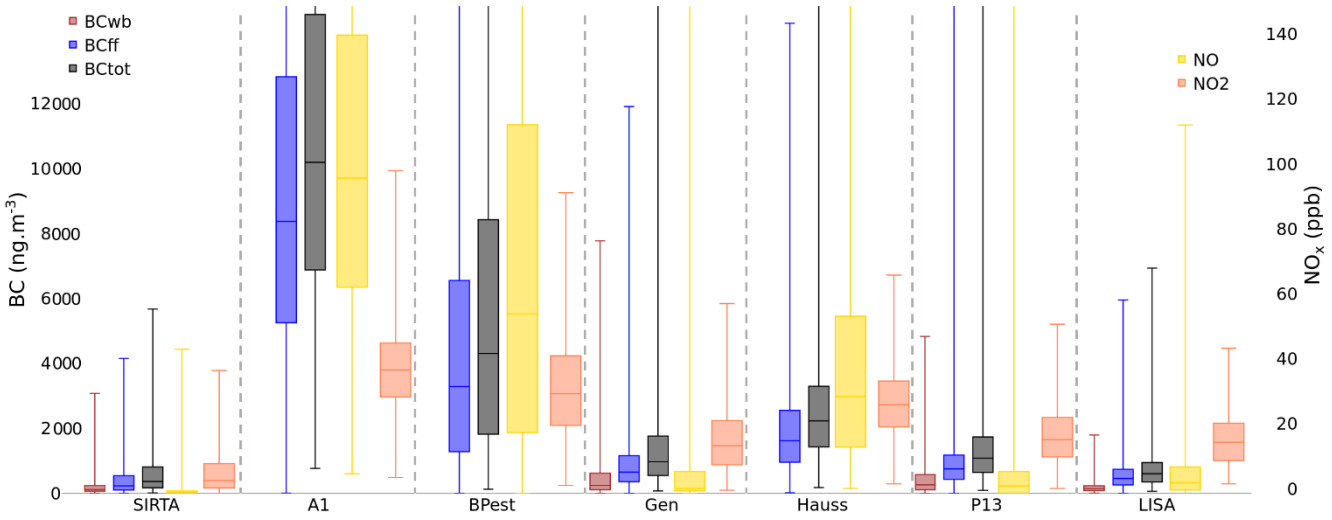

Figure K1 BC and NO_x measurements distribution for all the stations (A1, BPest, Gen, Hauss and P13 stand respectively for Highway A1, Ring road east, Gennevilliers, Boulevard Haussmann and Paris XIII^e). The box represents the upper and lower quartiles and the whiskers reach extreme values. The whole dataset was considered for SIRTA, the related period (Nov. 2017 – March 2018) was extracted from the long-term Airparif measurements and data from LISA is available for the shorter period (February – March 2018 as detailed in Section 2.2).

Appendix L: Correlation matrix for BC measurements

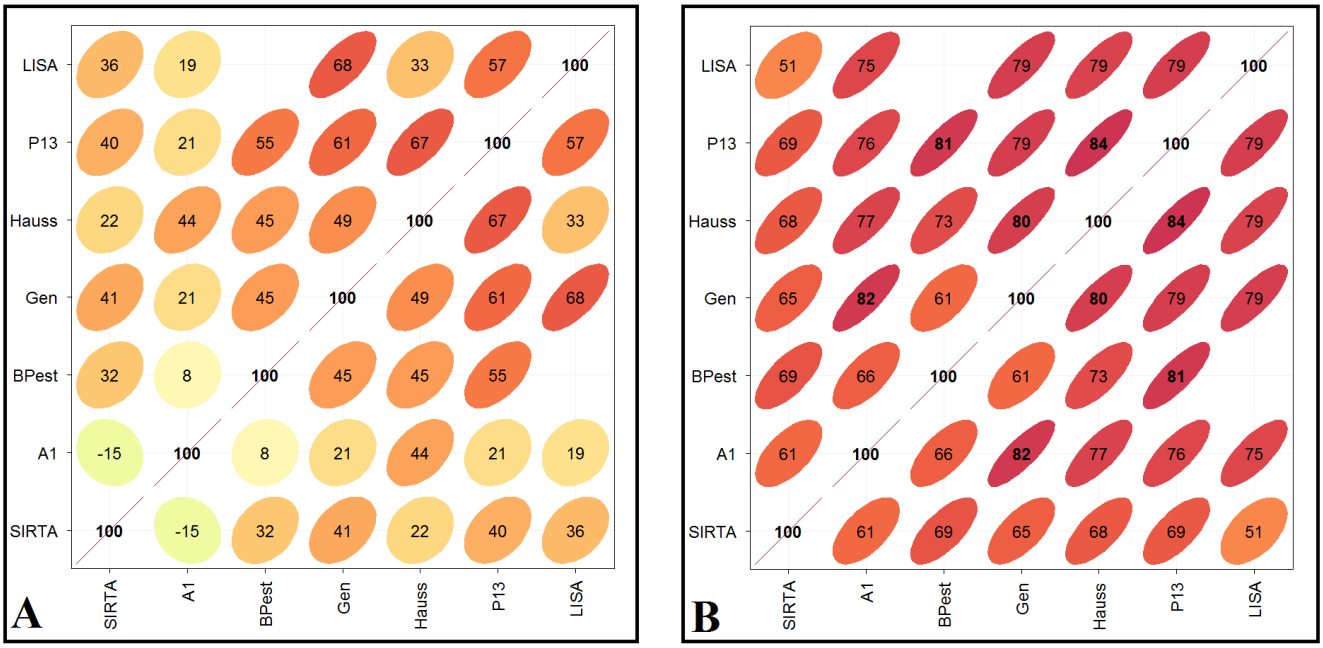

1185 **Figure L1 Correlation matrix for BC measurements from the SIRTA, Airparif and LISA stations. Box A is for $BC_{traffic}$ and box B for BC_{wb}. Presented values are the Pearson correlation coefficient multiplied by 100.**

Appendix M Correlation matrix – VOC

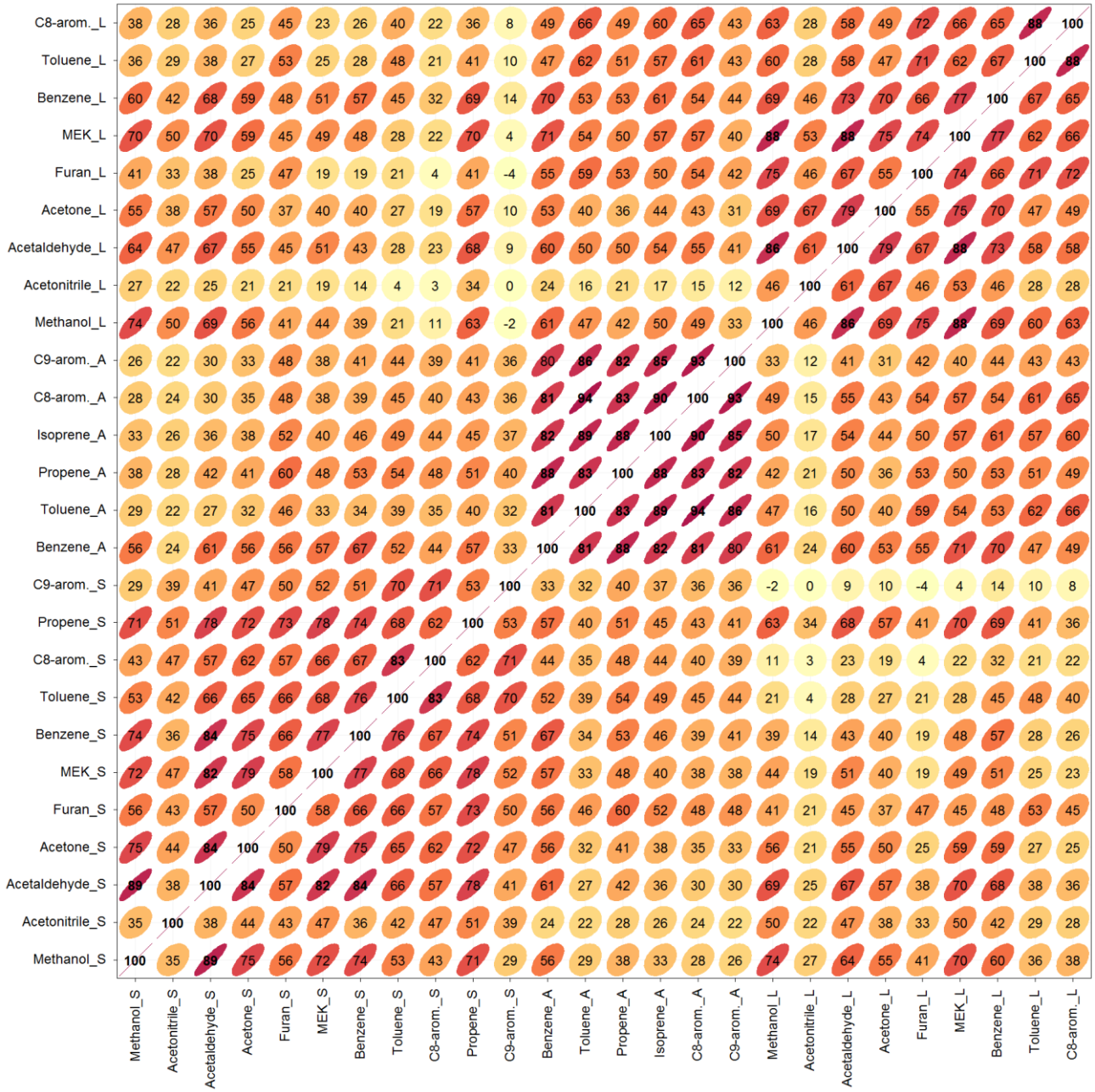

1190

Figure M1 Correlation matrix for the VOC measurements from the SIRTA, Airparif and LISA stations.

Appendix N: Association between temperature and wind speed

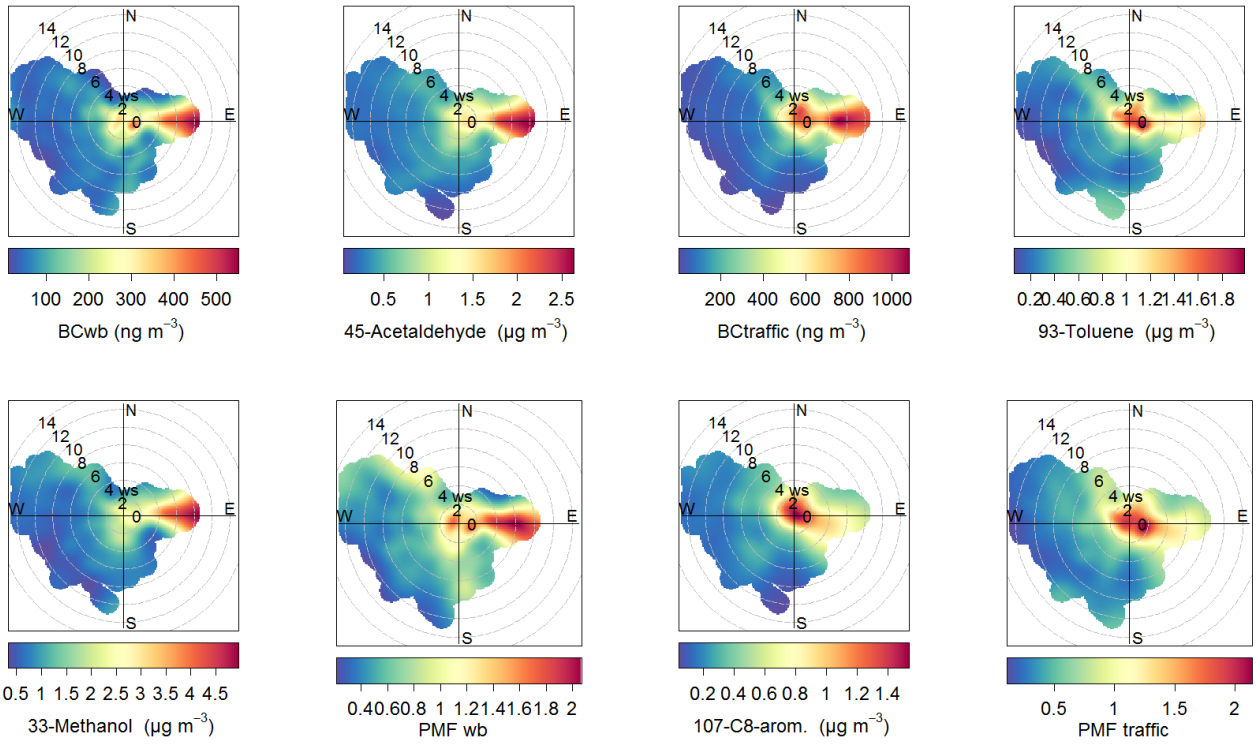

Figure N1 Polar plot of the concentrations as a function of wind (speed and direction) at SIRTA.

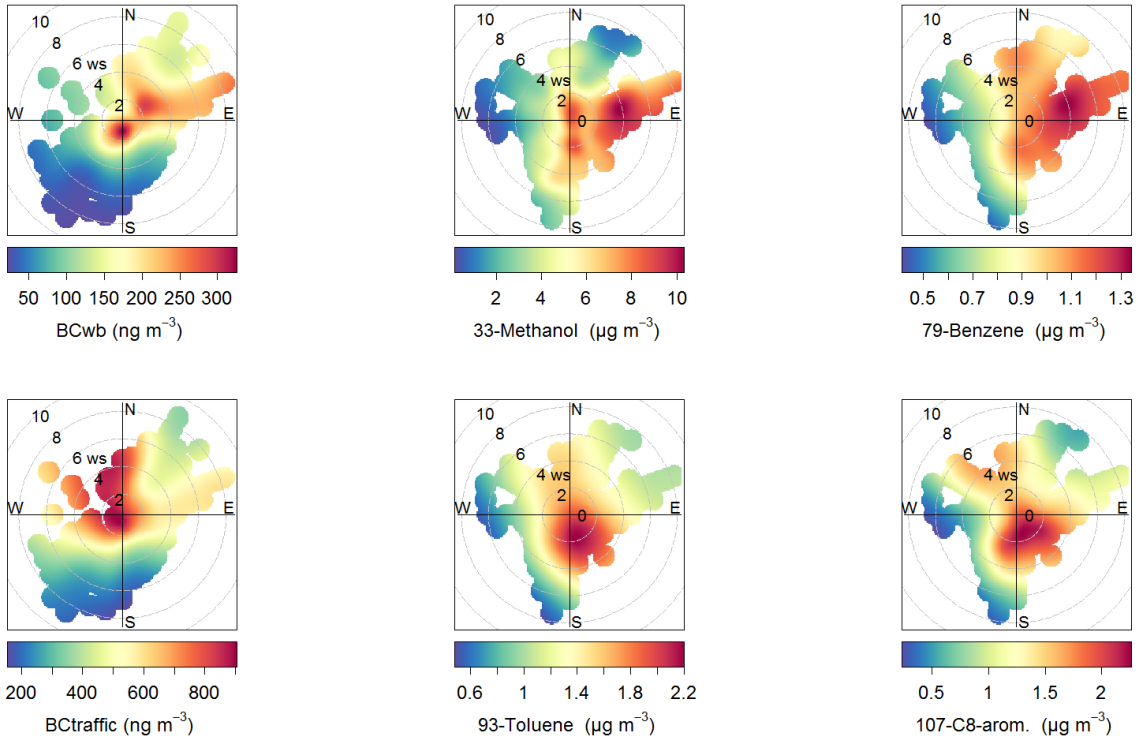

Figure N2 Polar plot of the concentrations as a function of wind (speed and direction) at LISA.

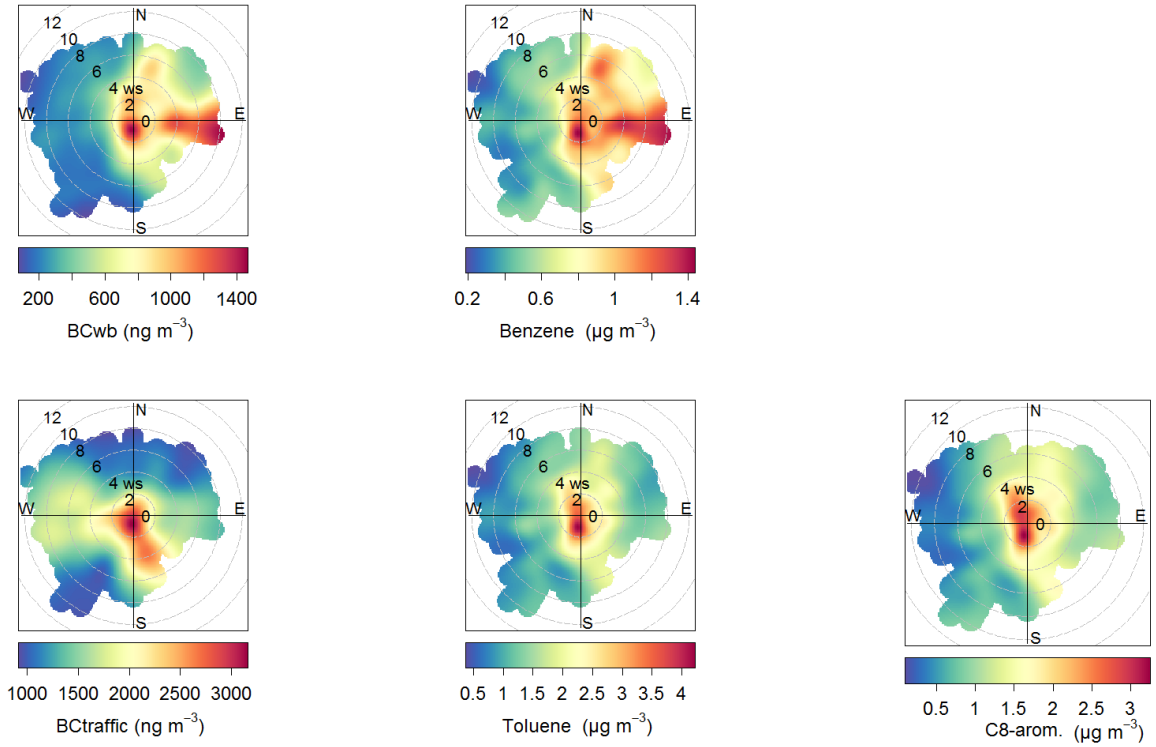

Figure N3 Polar plot of the concentrations as a function of wind (speed and direction) at Airparif.

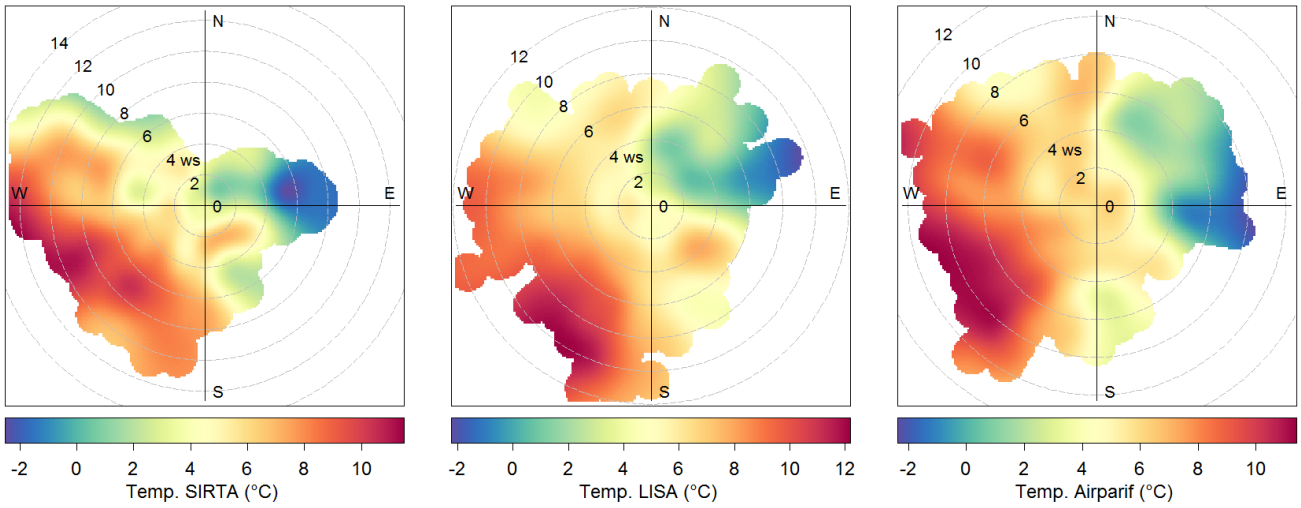

Figure N4 Polar plot of the association between temperature and wind (speed and direction) at the SIRTA, LISA and Airparif stations

Acknowledgements. This work has been supported by CNRS, CEA, DIM-QI2, H2020 ACTRIS project (grant agreement n° 654109). The authors acknowledge Patrick Garnoussi from Airparif, as well as Denis Fourgassié from Météo-France for providing several datasets necessary for the present study. Thank you to Marc Koenig from DRIEA Île-de-France for the traffic flow data. SNO-ICOS-France-Atmosphère provided the CO measurements. The authors gratefully acknowledge the NOAA Air Resources Laboratory (ARL) for the provision of the HYSPLIT transport and dispersion model used in this publication. The authors also acknowledge Renaud Falga for his work on the preliminary data processing and analysis.